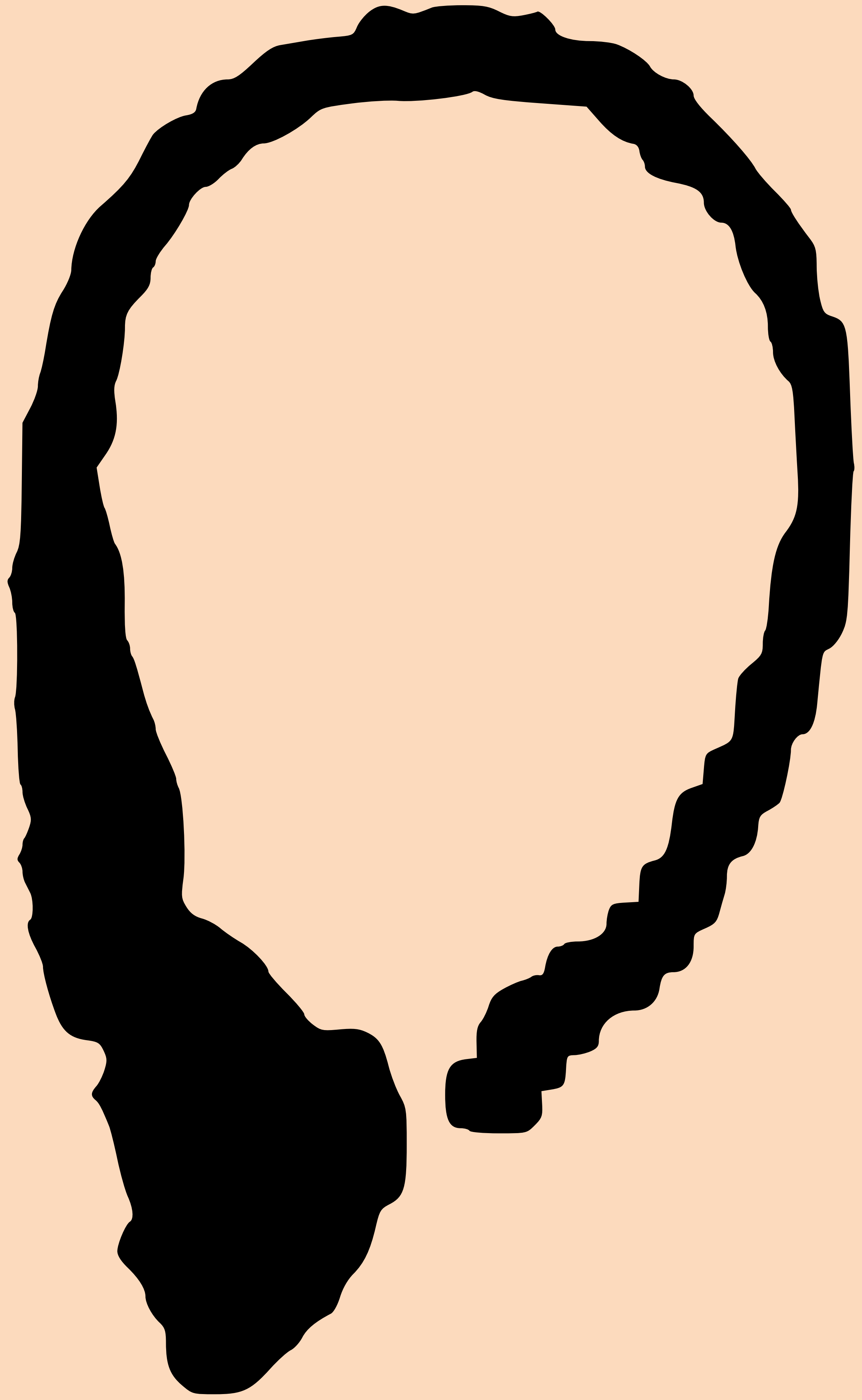

Fast Radio Bursts as Precursor Radio Emission from Monster Shocks

Arno Vanthieghem

In collaboration with **Amir Levinson** (TU)

Workshop: Kinetic physics of astrophysical plasmas

June 18-20, 2025

Fast Radio Bursts main properties

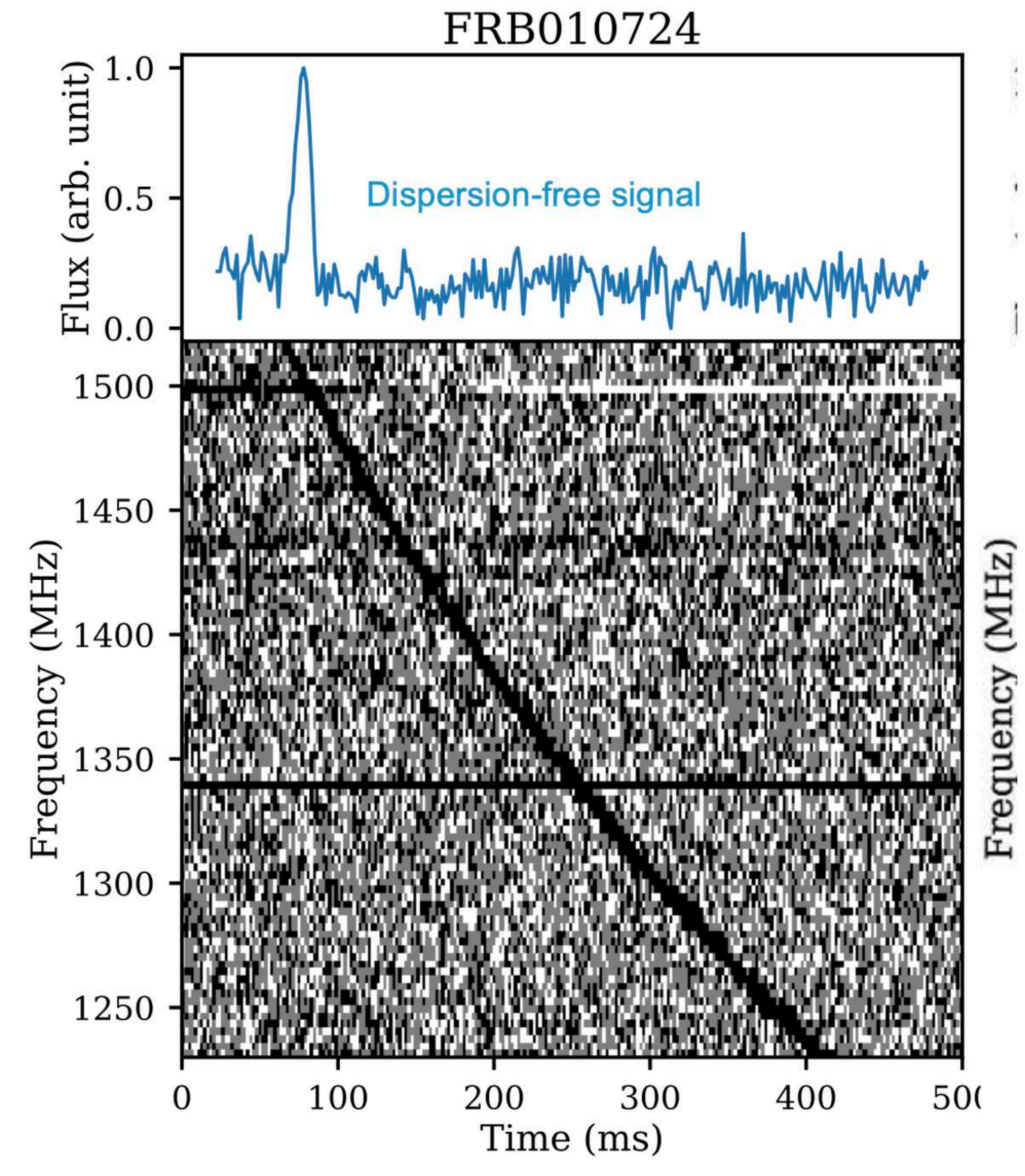

Lorimer et al., 2007

Some properties:

- First detection in 2007 (from 2001's catalogue)
- Short pulse: ~1ms
- Radio band: 0.1 to 8 GHz
- Bright radio sources: 1 – 100 Jy (Cas A ~ 2000 Jy at 1 GHz)
- Large all-sky rate: 10^3 -10^4 sky^{-1} day^{-1} above 1 Jy ms-fluence
- Large DM [$t_\mathrm{d} \simeq 4.15\,\mathrm{ms}\left(\frac{\mathrm{DM}}{\nu^2}\right)$, ν in GHz, Dispersion Measure $\mathrm{DM} = \int_{src}^{obs} n_e\,\mathrm{d}s$ [pc cm^{-3}]]
- Repeating (> 50) or not ($\gg 500$), with spectral features (sad trombone) or not

Fast Radio Bursts are cosmological

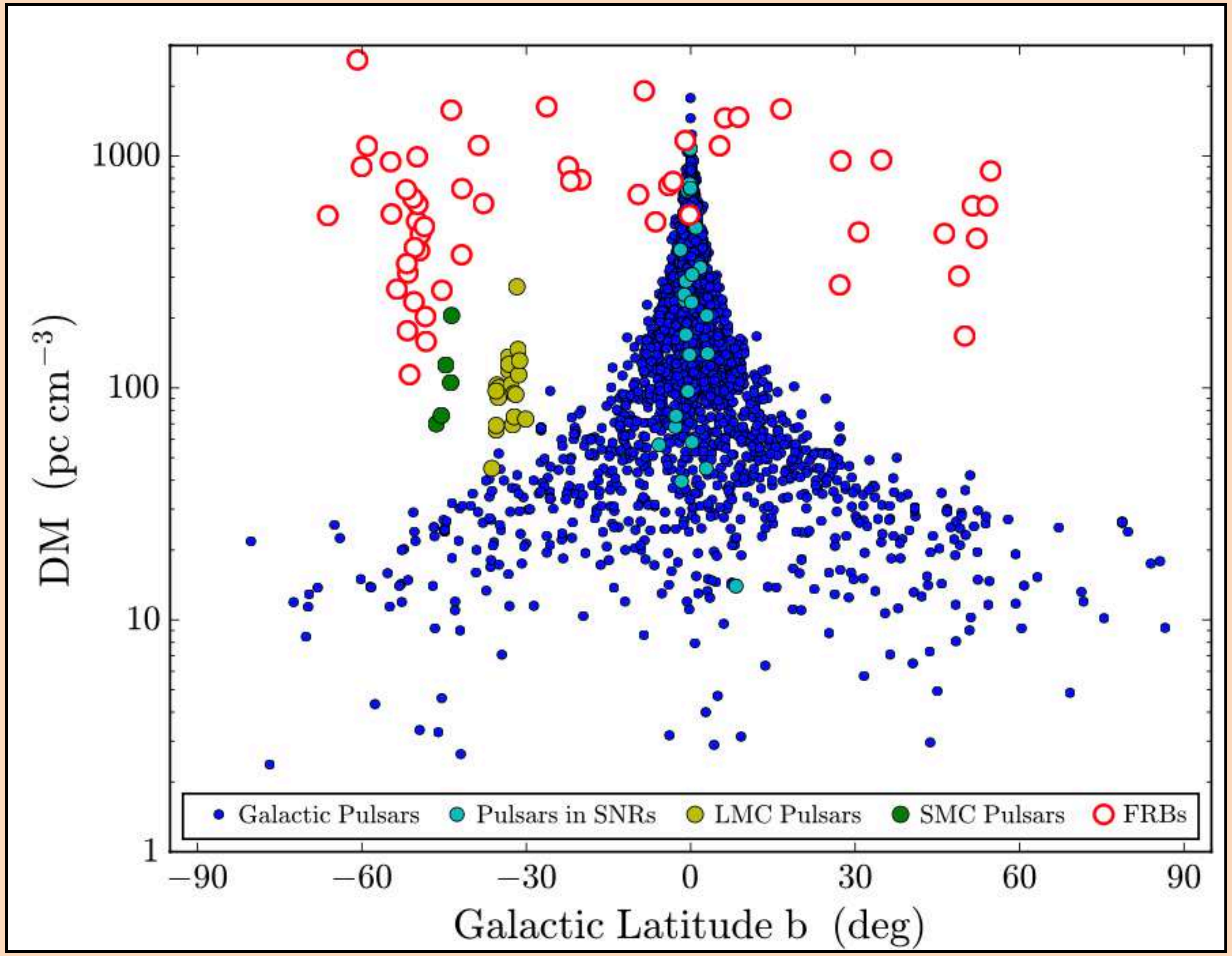

Cordes, Chatterjee 2020

Observations show FRBs to be of extragalactic origin ($z \sim 0.03 - z \geq 1$) with a distribution that seems to be isotropic

5 FRBs localized in a host galaxy at distances 10^8–10^9 ly (distance to Andromeda Galaxy ~10^6 ly) - *i.e.* cosmological scales

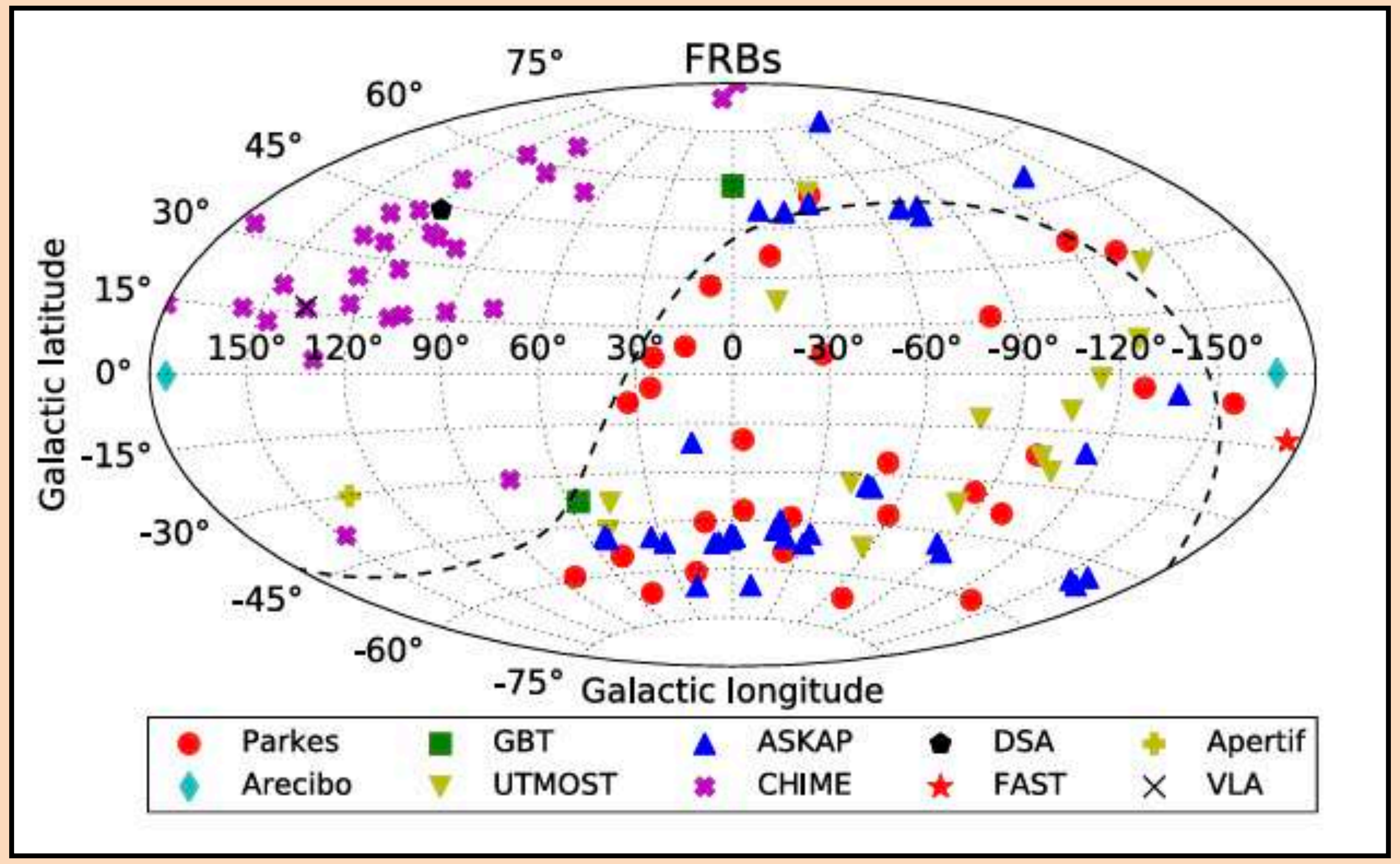

Most FRBs show linearly polarized emission

Observatoire de Paris

rFRB 20180301A

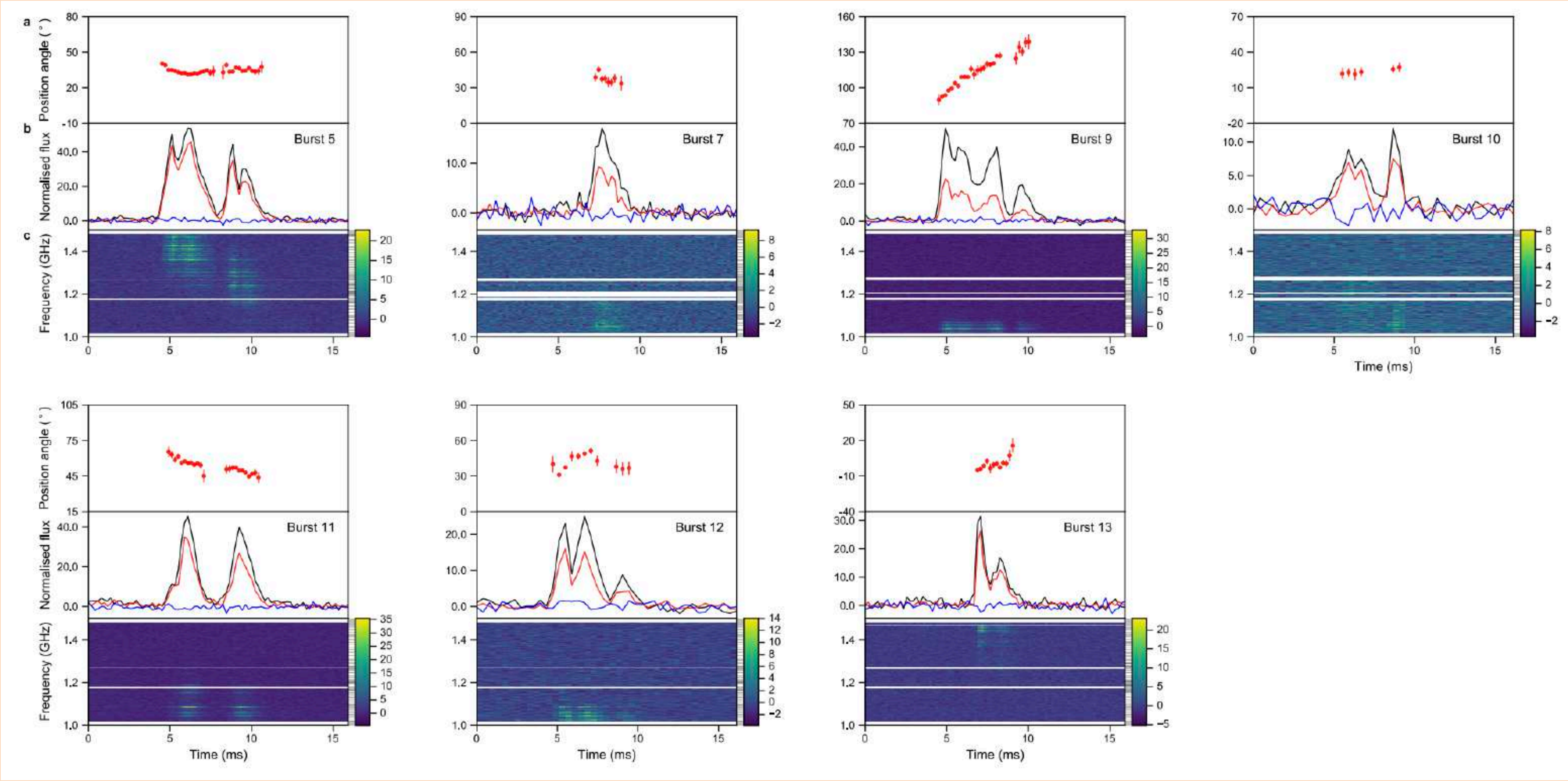

Luo et al. 2020

rFRB 20121102A

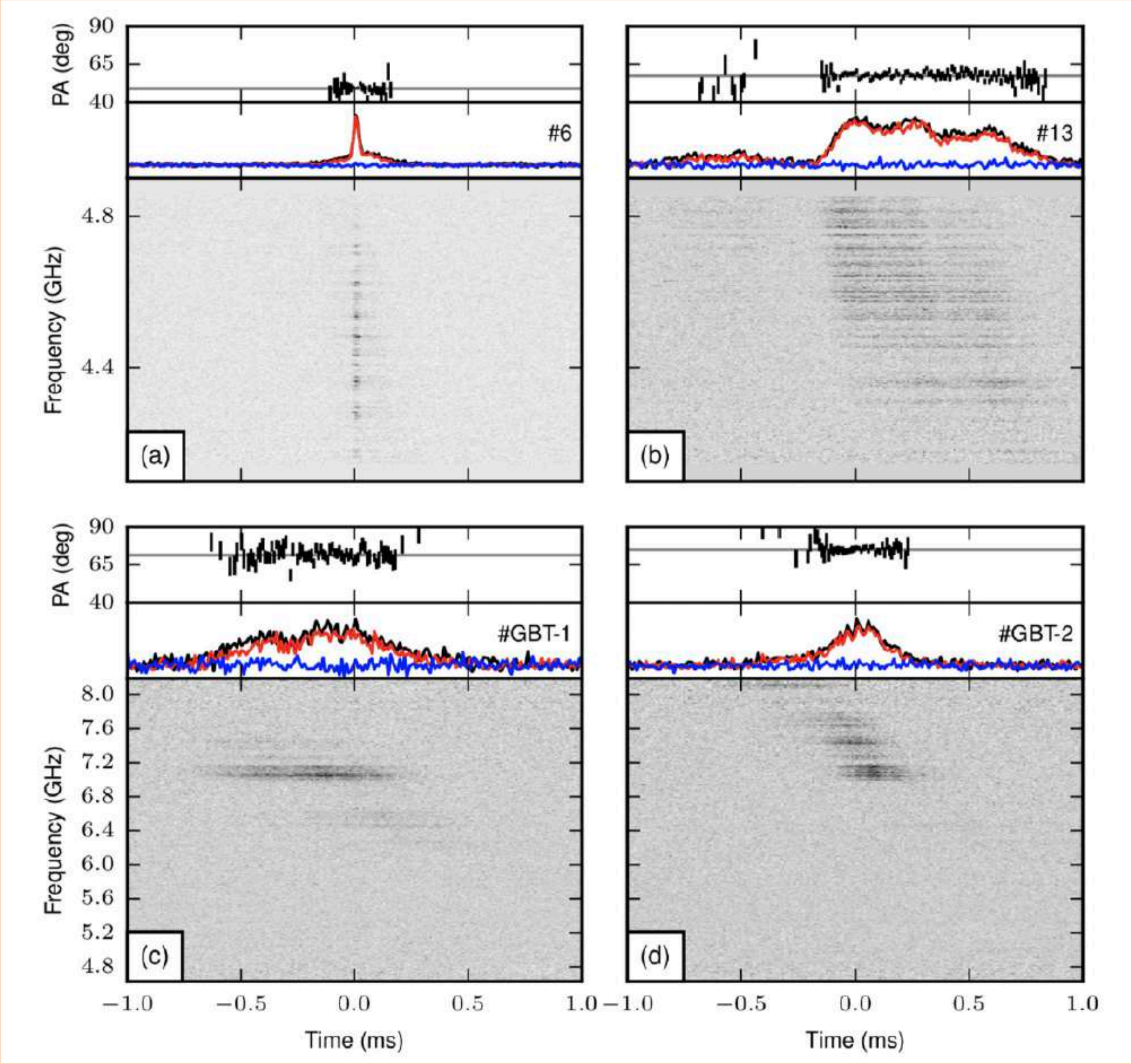

Michilli et al. 2018

FRB20221022A

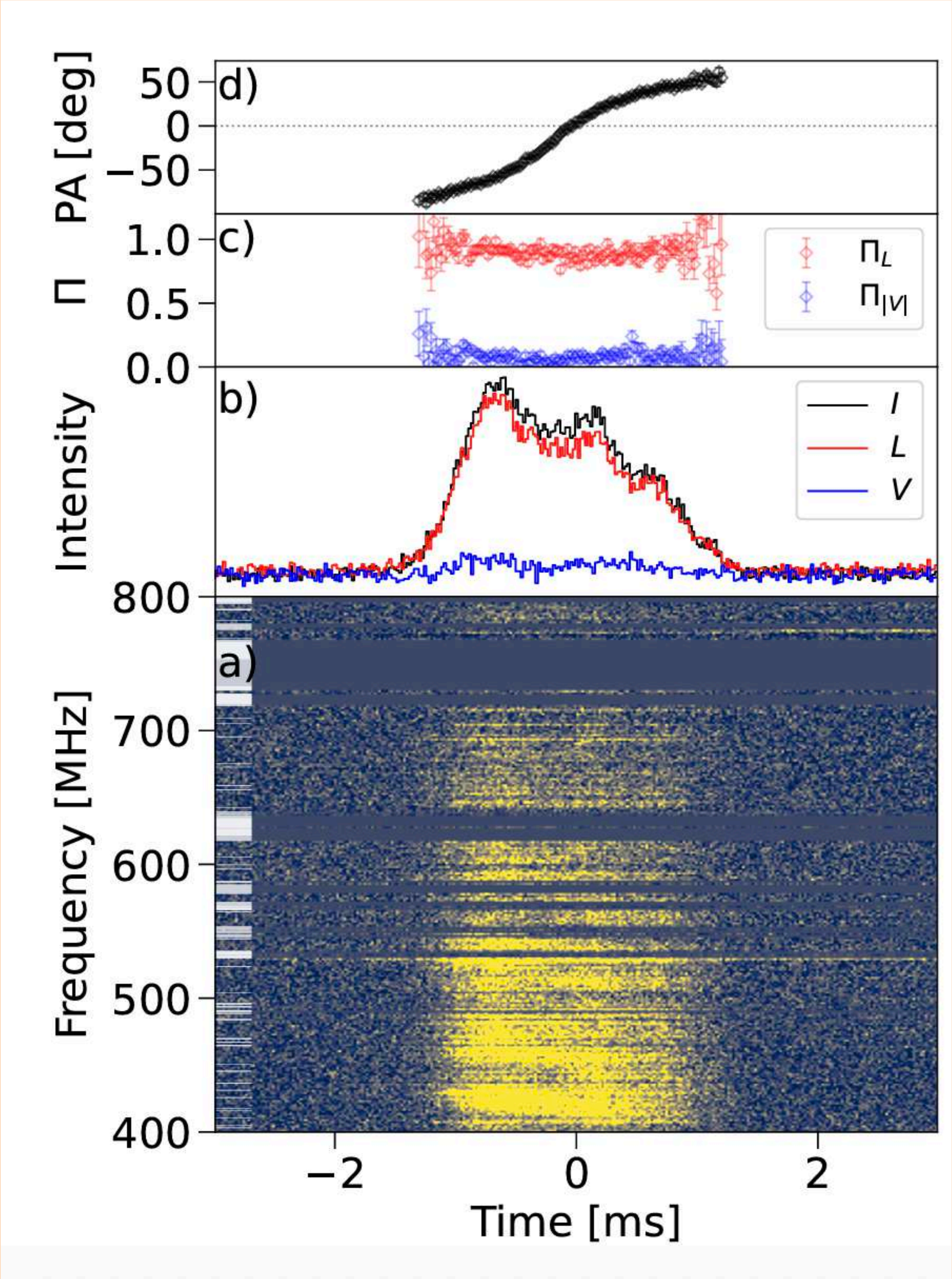

Mckinven et al. 2024

- Strong linear polarization in both repeating and one-off

- Some show swings in the polarization angle (both for repeating and one-off) suggesting propagation in strong B-field

$$\mathrm{RM} = (-0.81\,\mathrm{rad\,m^{-2}}) \int_0^{D_z} \frac{B_\parallel/\mu\mathrm{G}\, n_e}{(1+z)^2} \mathrm{d}l$$

Many potential sources… Magnetars emerge as ideal candidates.

At least some FRBs are produced by Magnetars

Magnetar X-ray bursts …

Gögüs et al. 1999, 2000, 2001; Rea et al., 2009; Rea & Esposito, 2010; Kaspi & Beloborodov, 2017; Esposito et al., 2020

from twisted magnetospheres

Parfrey et al. 2013; Mahlmann et al. 2019; Yuan et al. 2020; Sharma et al. 2023

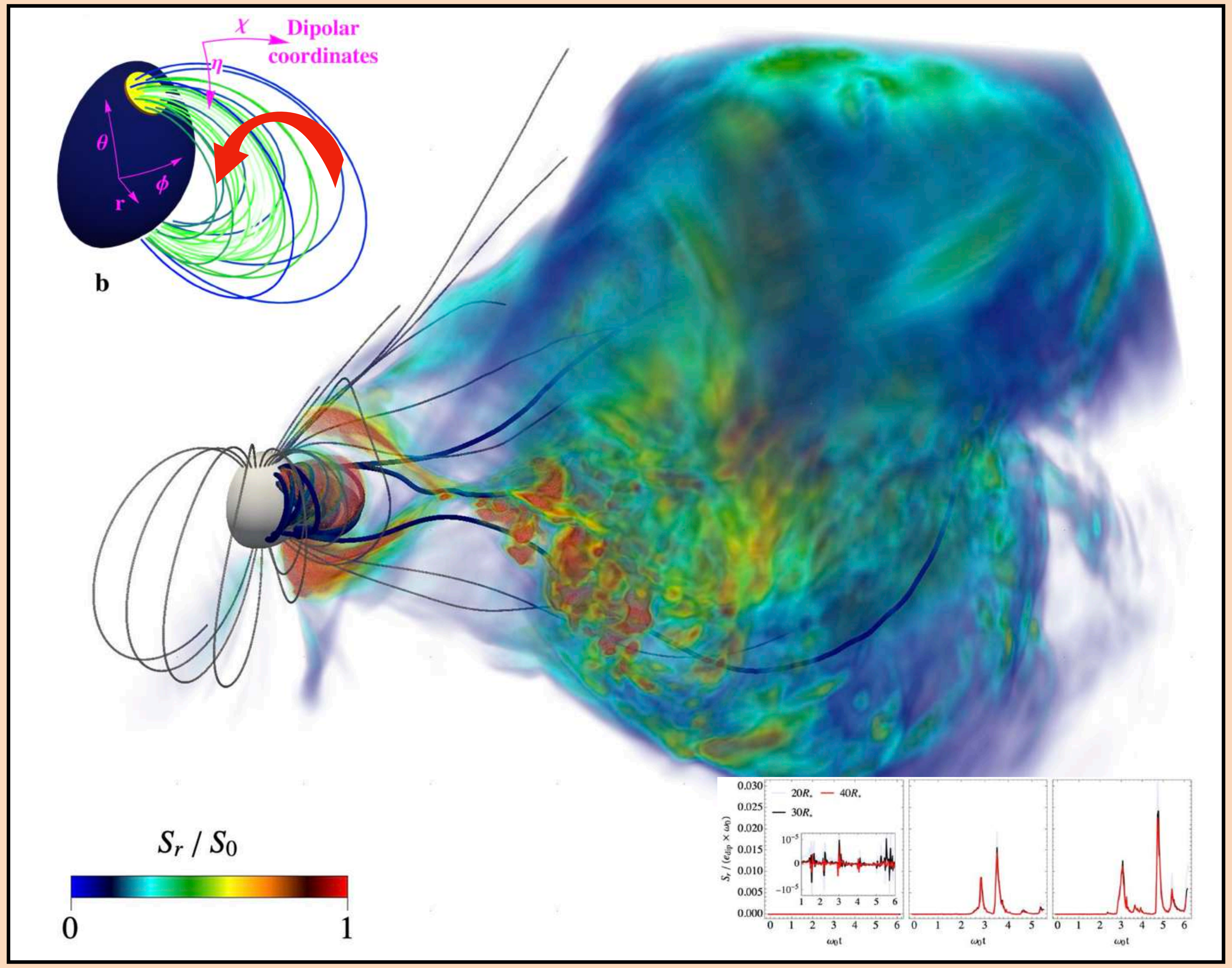

Mahlmann et al., 2023

FRB 200428 + hard X-rays from SGR 1935+2154

CHIME/FRB Collaboration, 2020; Bocheneck et al., 2020; Ridnaia et al., 2021

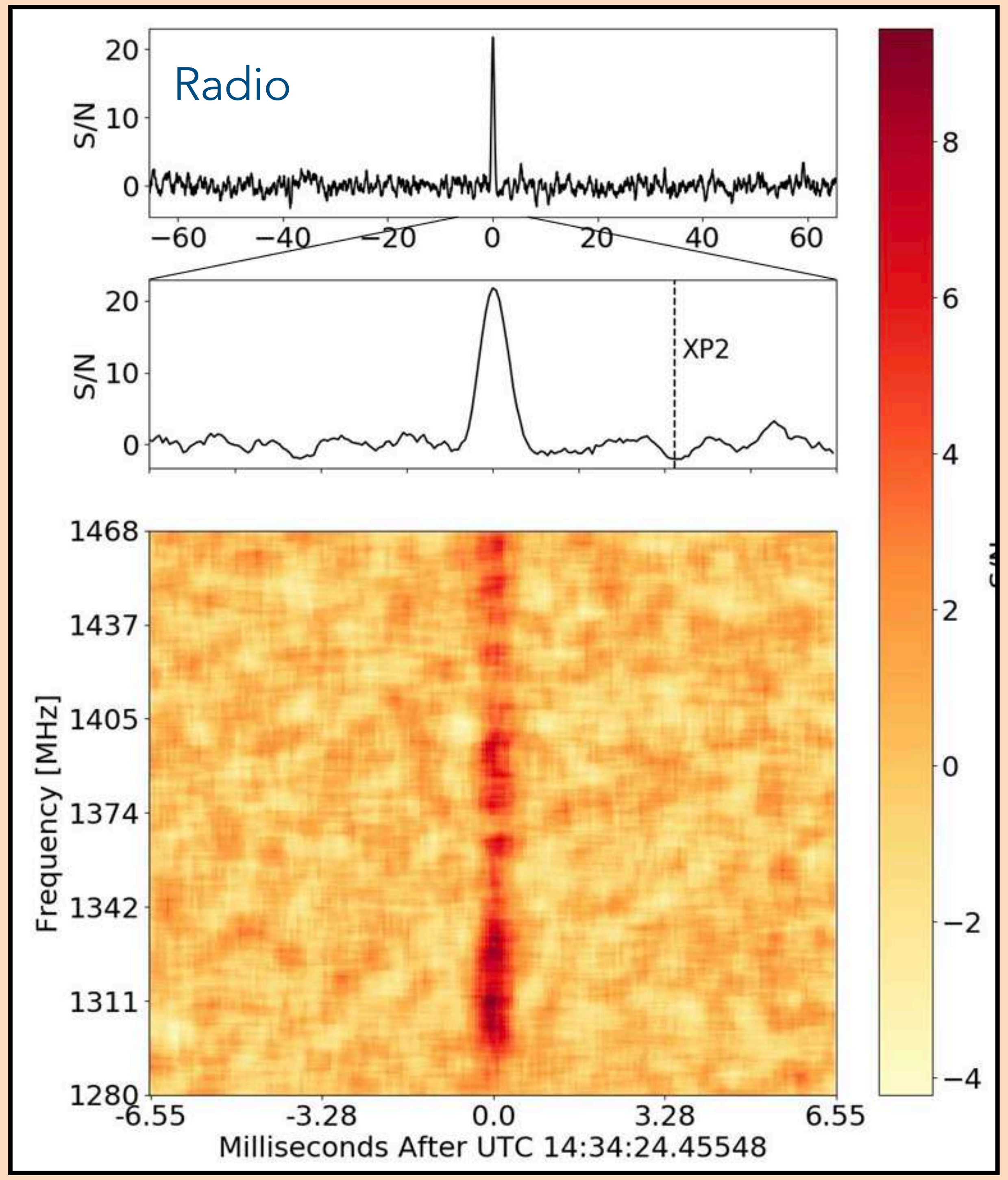

Bocheneck et al., 2020

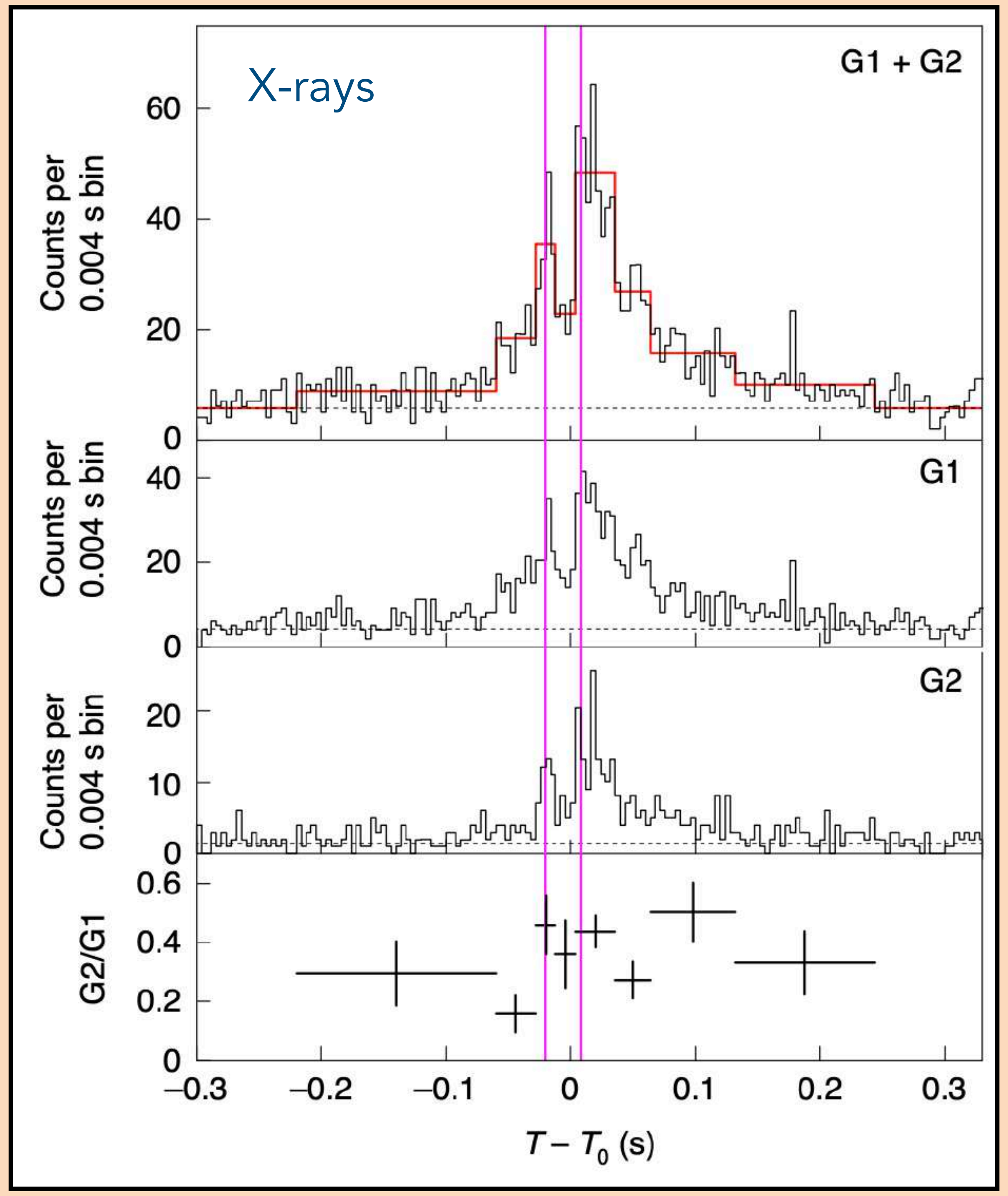

Ridnaia et al., 2021

Two main categories of FRBs emission mechanisms

Observatoire de Paris

Far-away models

FRB is emitted very far from the neutron star and outside the magnetosphere. An ejecta propagates away from the magnetosphere, collides with the external medium, and generates a shock responsible for the FRB emission.

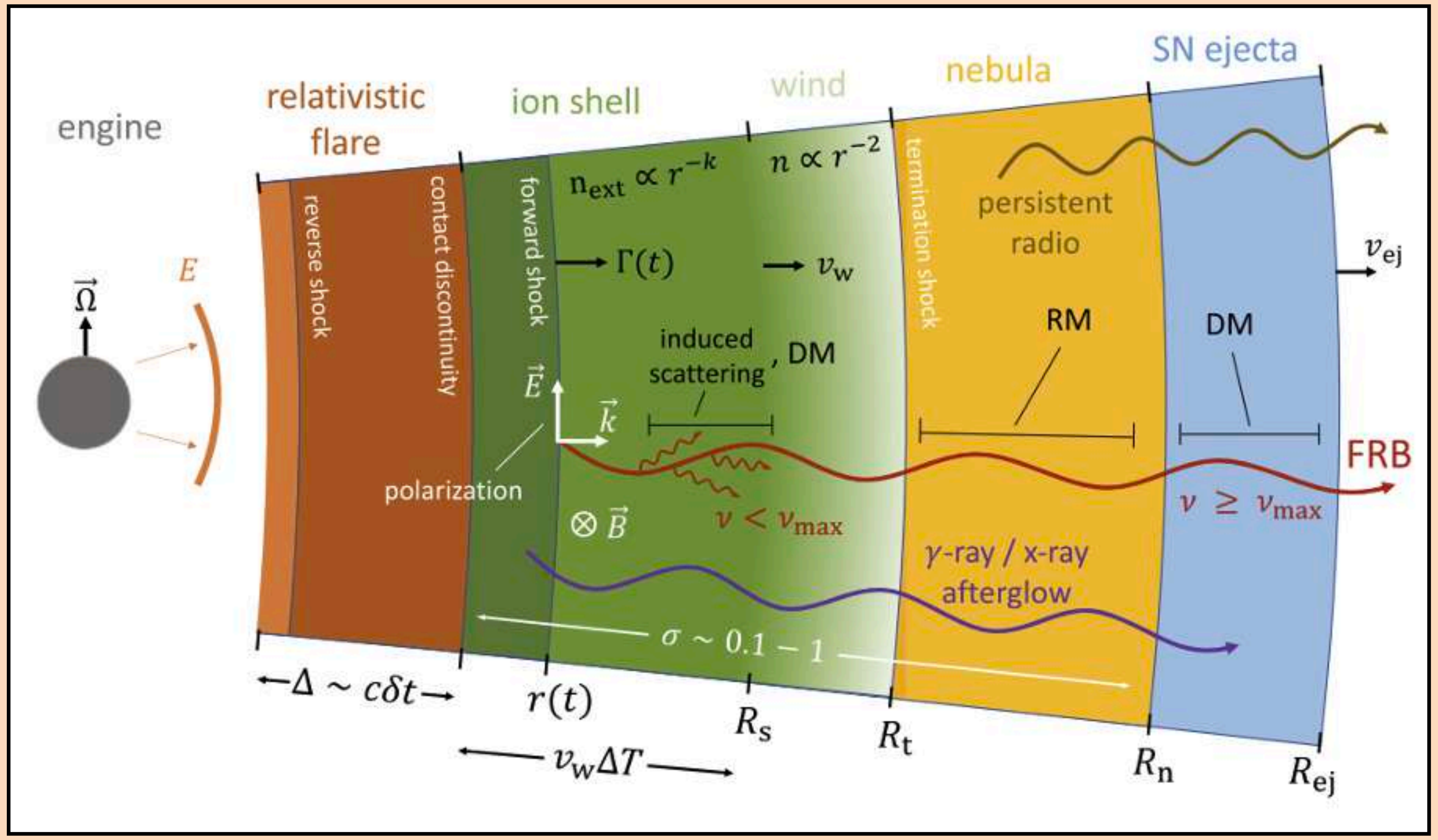

Metzger et al., 2019

Inner magnetospheric emission models

Emission originates from the inner magnetosphere through various plasma processes, such as magnetic reconnection and shocks.

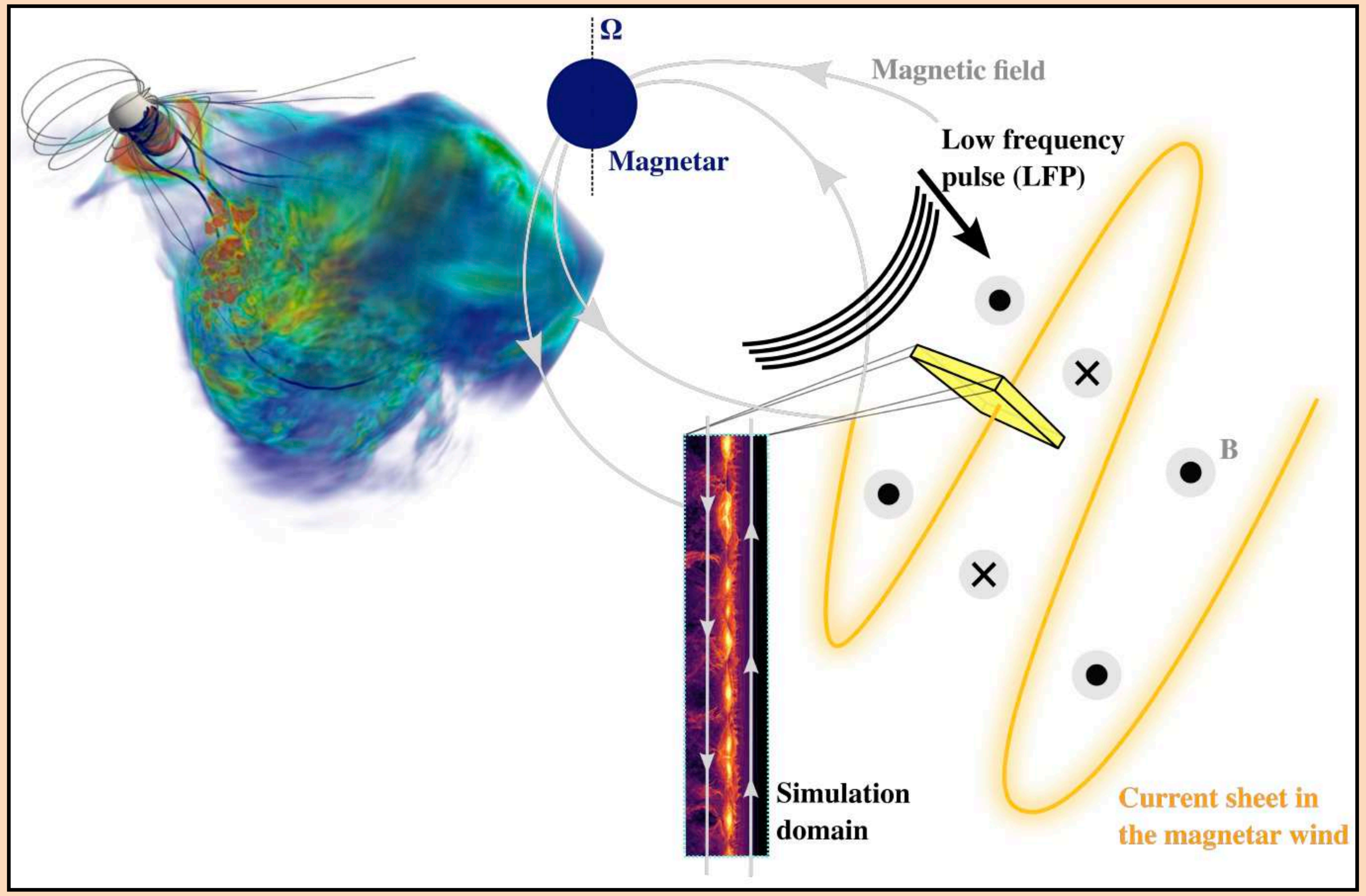

Mahlmann et al., 2022, 2023

Some observations seem to favor a magnetospheric origin for some FRBs: scintillation (Nimmo et al., 2025), change of the PA (Luo et al., 2020), phenomenological fitting (Voisin et al., to be submitted) with emission radius about $\sim 10^2\,R_s$

Two main categories of FRBs emission mechanisms

Observatoire de Paris

Far-away models

FRB is emitted very far from the neutron star and outside the magnetosphere. An ejecta propagates away from the magnetosphere, collides with the external medium, and generates a shock responsible for the FRB emission.

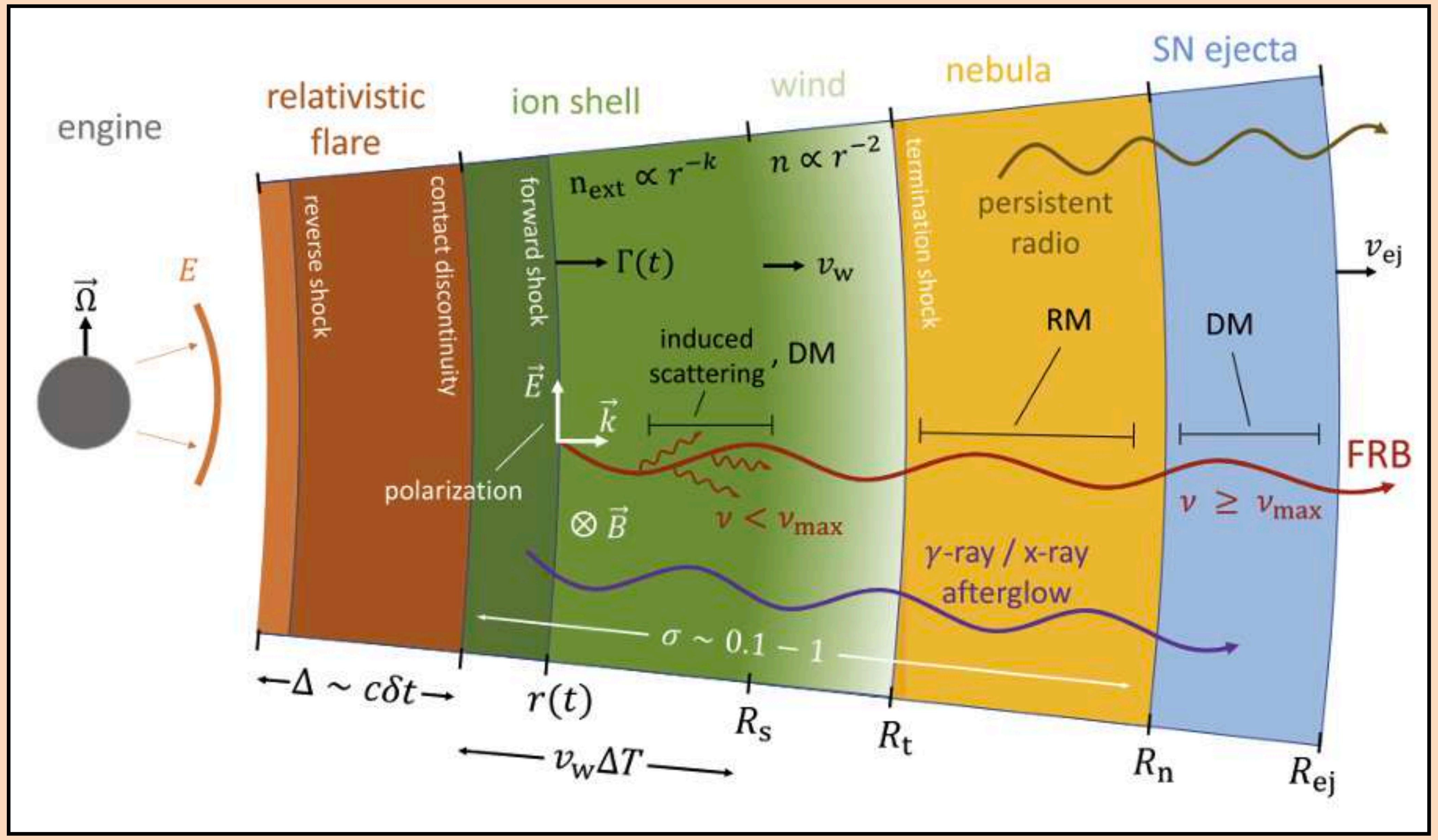

Metzger et al., 2019

Inner magnetospheric emission models

Emission originates from the inner magnetosphere through various plasma processes, such as magnetic reconnection and shocks.

This work

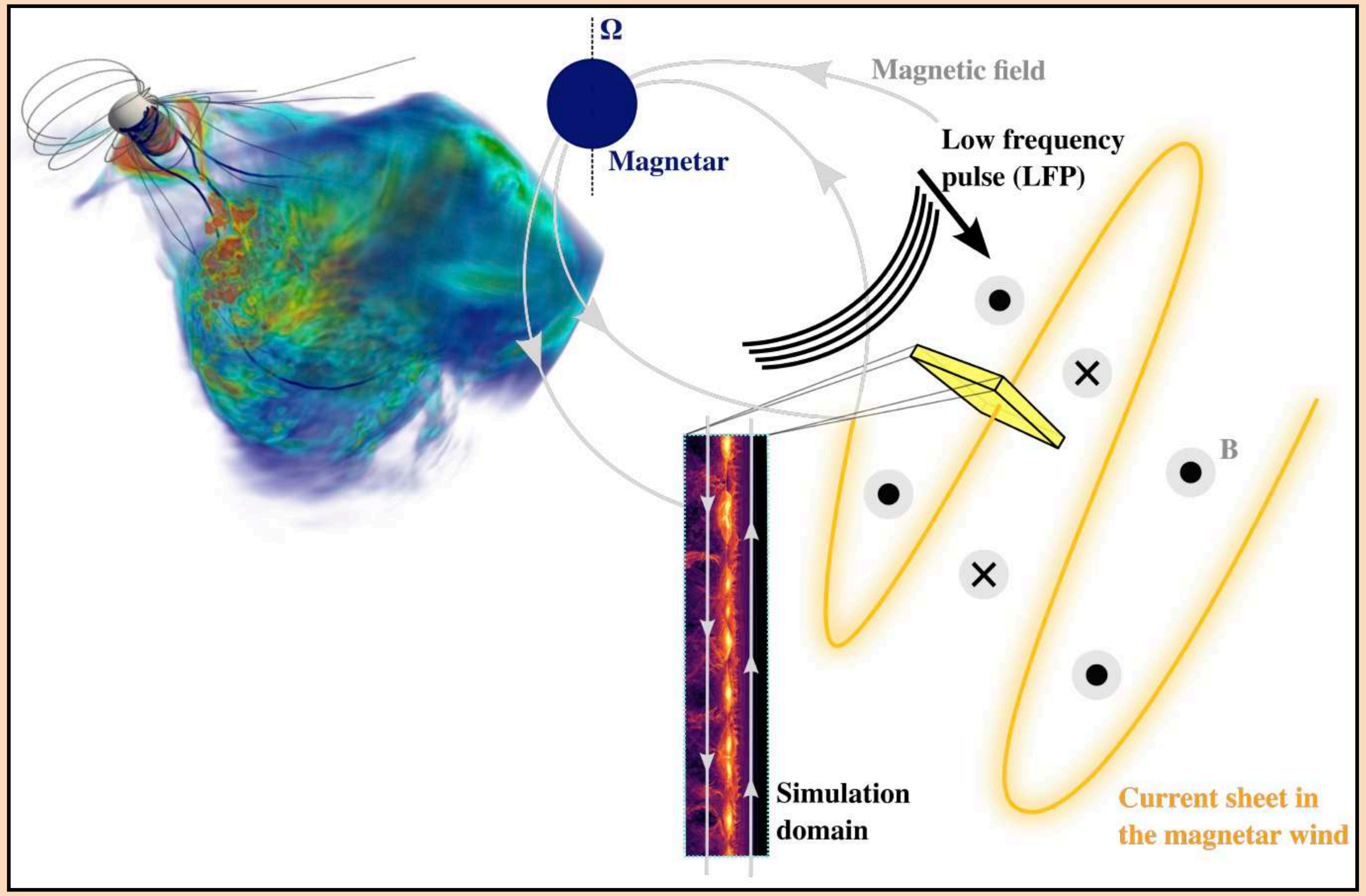

Mahlmann et al., 2022, 2023

Some observations seem to favor a magnetospheric origin for some FRBs: scintillation (Nimmo et al., 2025), change of the PA (Luo et al., 2020), phenomenological fitting (Voisin et al., to be submitted) with emission radius about $\sim 10^2\, R_s$

MHD Waves in Twisted Magnetospheres

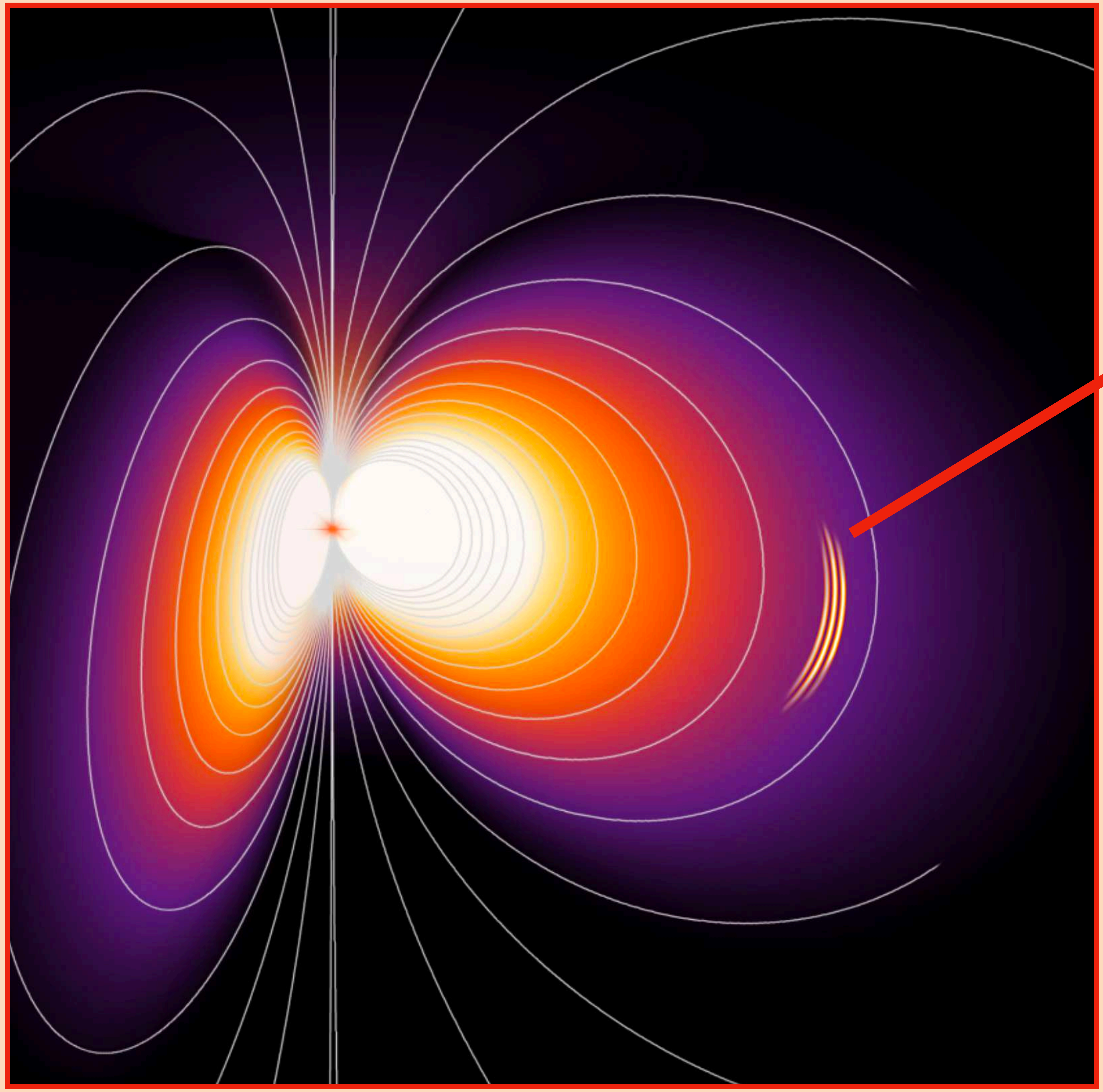

Force-free magnetosphere: $\mathbf{E} \cdot \mathbf{B} = 0, \qquad \sigma = \frac{B_{bg}^2}{4\pi\rho c^2} \gg 1$

- **Alfven wave:** Along the field lines $B_w \propto k \times B_{bg}$
- **Compressive Fast Magnetosonic Wave (This Presentation)**

  Across the field lines $E_w \propto k \times B_{bg}$

We expect three regimes of interest, dictated by the $B^2 - E_w^2$

1. $B^2 - E_w^2 \gg 0$ A small linear wave is injected
2. $B^2 - E_w^2 \to 0$: **A strongly nonlinear wave at sufficiently large radius** (This Presentation)
3. $B^2 - E_w^2 < 0$: Formation of an electric zone [Alfvén wave collision (Xinyu et al., 2019, Li et al., 2021), monster shocks (Chen et al., 2022)]

Steepening of a Fast Magnetosonic Wave

Observatoire de Paris

Fate of a FMS wave (E_w, B_w) propagating in a declining background field B_{bg} (total: $B = B_{bg} + B_w$)

- Propagation: $E_w/B_{bg} \propto r^n$ (dipole: $E_w/B_{bg} \propto r^2$) $\Rightarrow$ $(B^2 - E_w^2 > 0)$ progressively $(B^2 - E_w^2 \to 0)$ at the trough

$\Longrightarrow$ **Formation of a monster shock** [PIC: Chen et al., 2022; Theory (dipole in the high-σ limit): Beloborodov, 2023]

Exact 1D MHD-solution in a cold plasma + kinetic simulation of the shock formation & emission

- Large scale separation: $\lambda_w \omega_p/c = 10^4$
- Background field profile: $\mathbf{B}_{bg} = \hat{z}\, B_0(1 + x/R_0)^{-1}, \quad R_0 = 10\,\lambda_w$
- Large magnetization: $\sigma_{bg} = \sigma_0(1 + x/R_0)^{-2}, \quad \sigma_0 = 1600$
- Coolingdiscussed later
- 60 cells per skin depth, PPC = 100

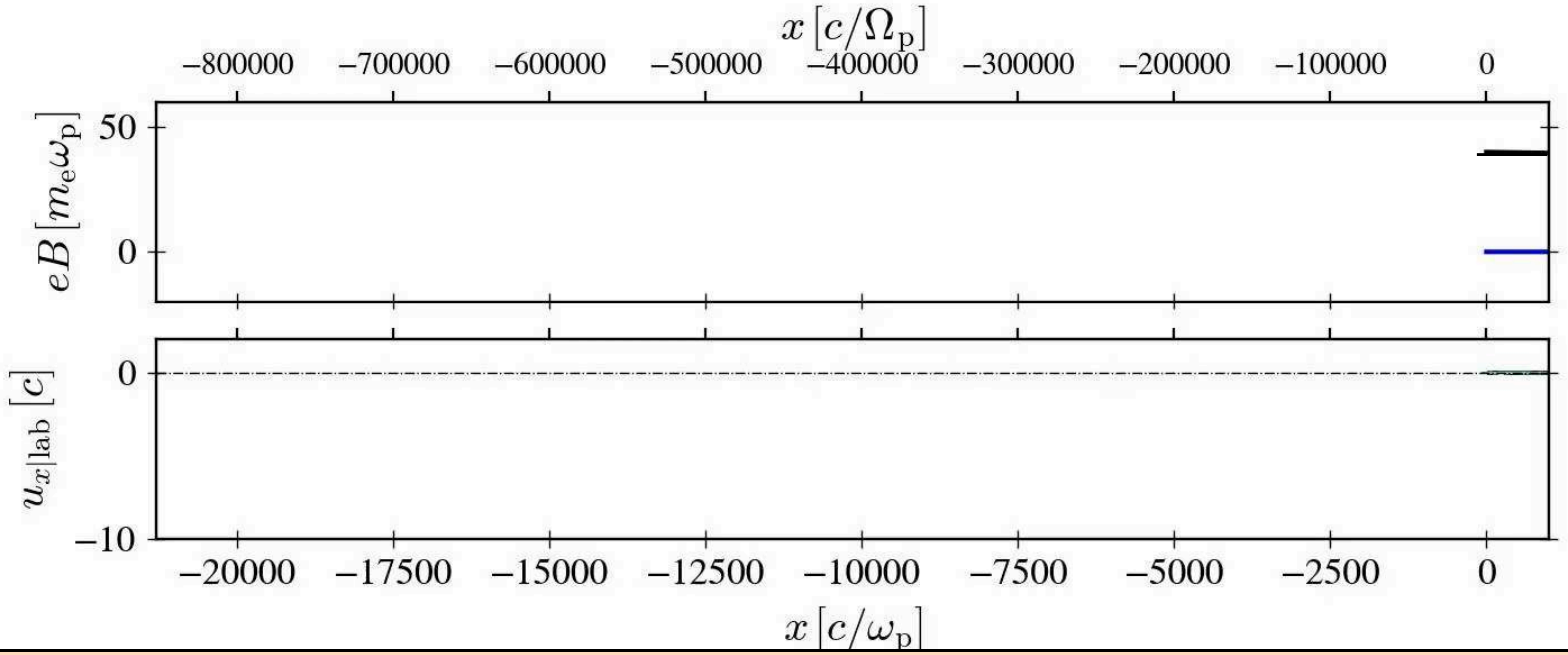

A. Vanthieghem & A. Levinson, PRL, 2025

Dissipation in a Strongly Magnetized Relativistic Shocks

Observatoire de Paris

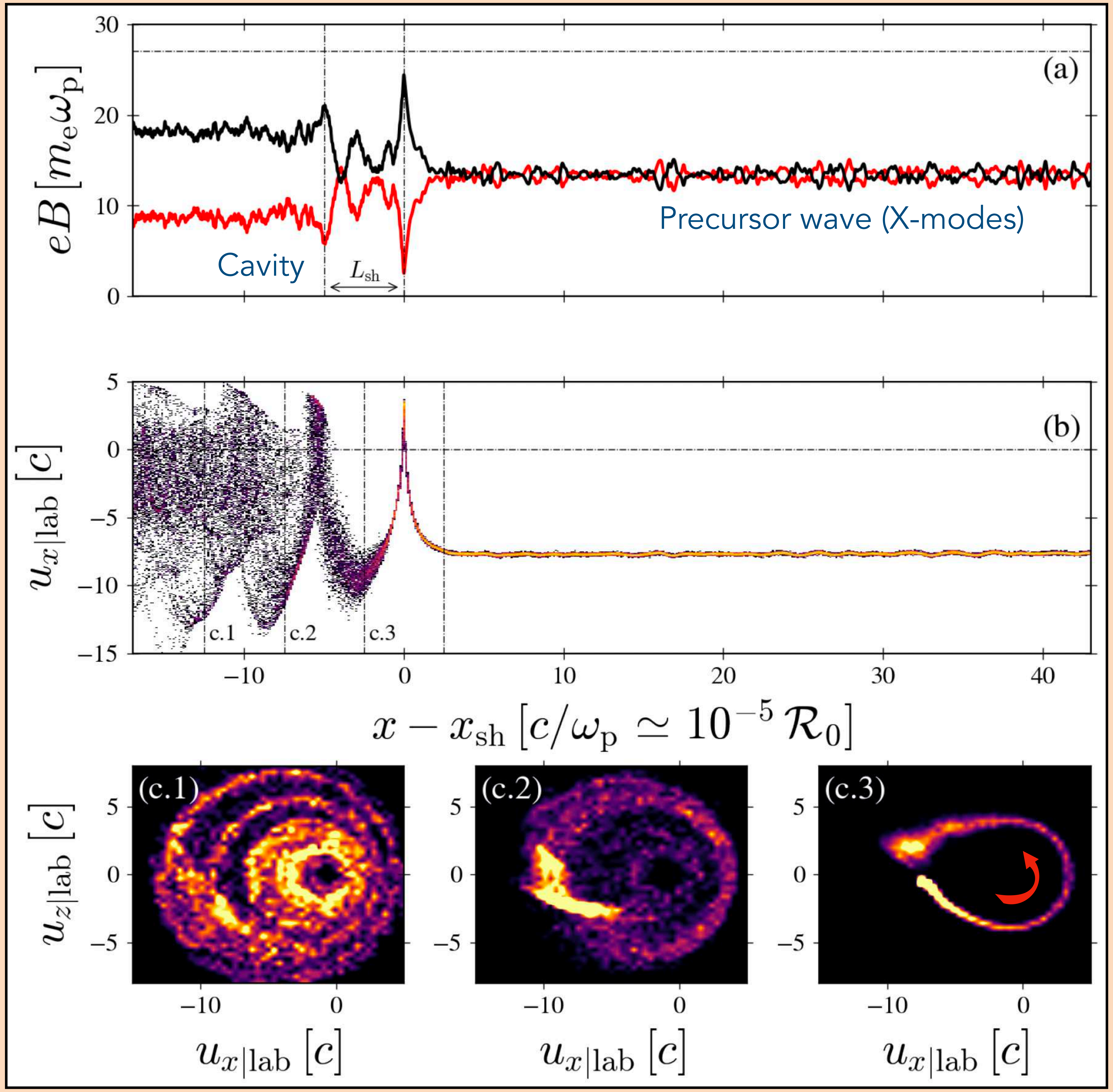

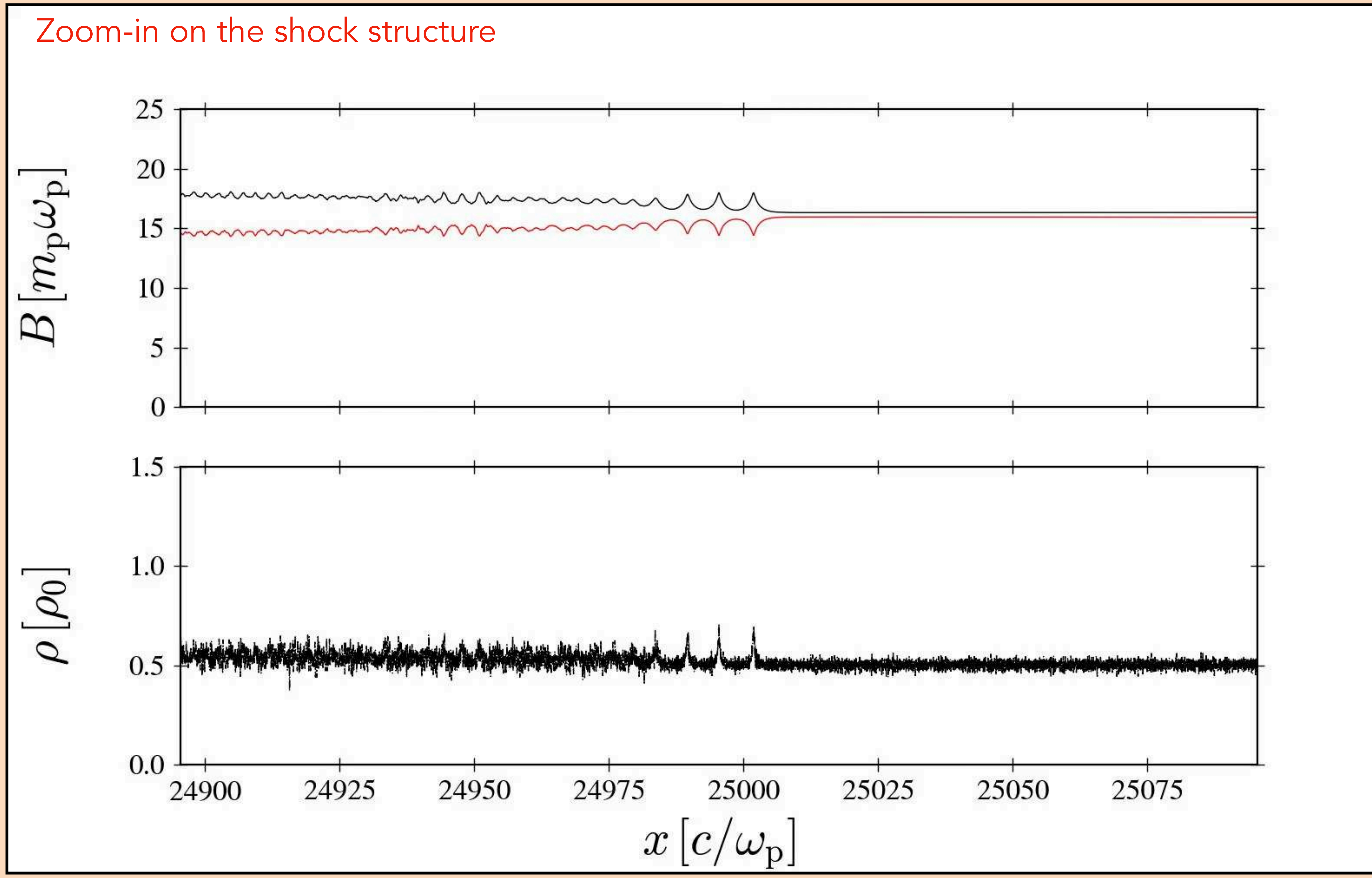

- **Excitation of a precursor wave** Planar shocks simulations: Iwamoto et al., 17-18; Plotnikov & Sironi 19; Sironi et al., 21; Babul et al., 21
- **Emission: Synchrotron-Maser in a resonant cavity** (Plotnikov et al., 19)?

A. Vanthieghem & A. Levinson, PRL, 2025

Spectrum and Dissipation Rate

Observatoire de Paris

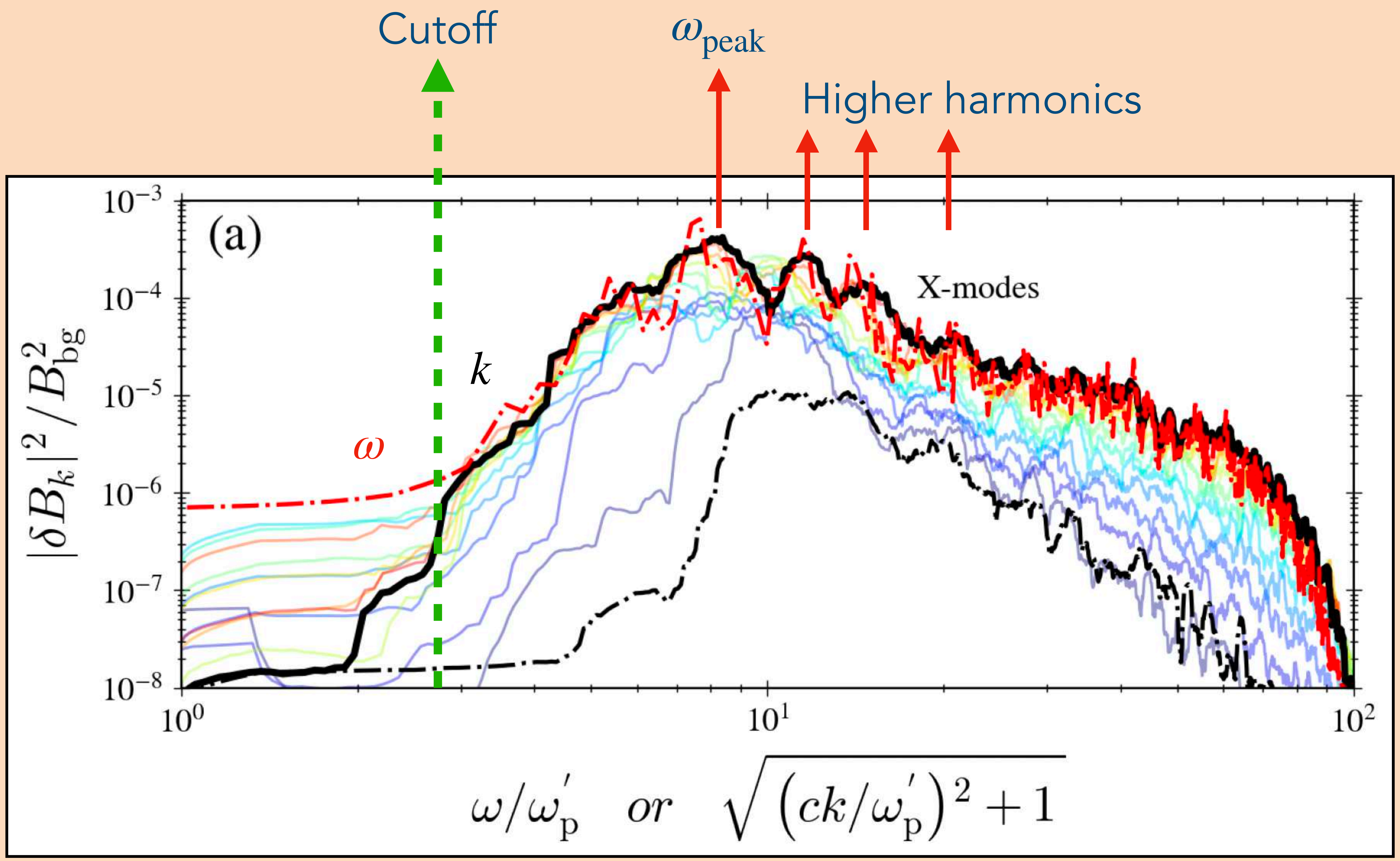

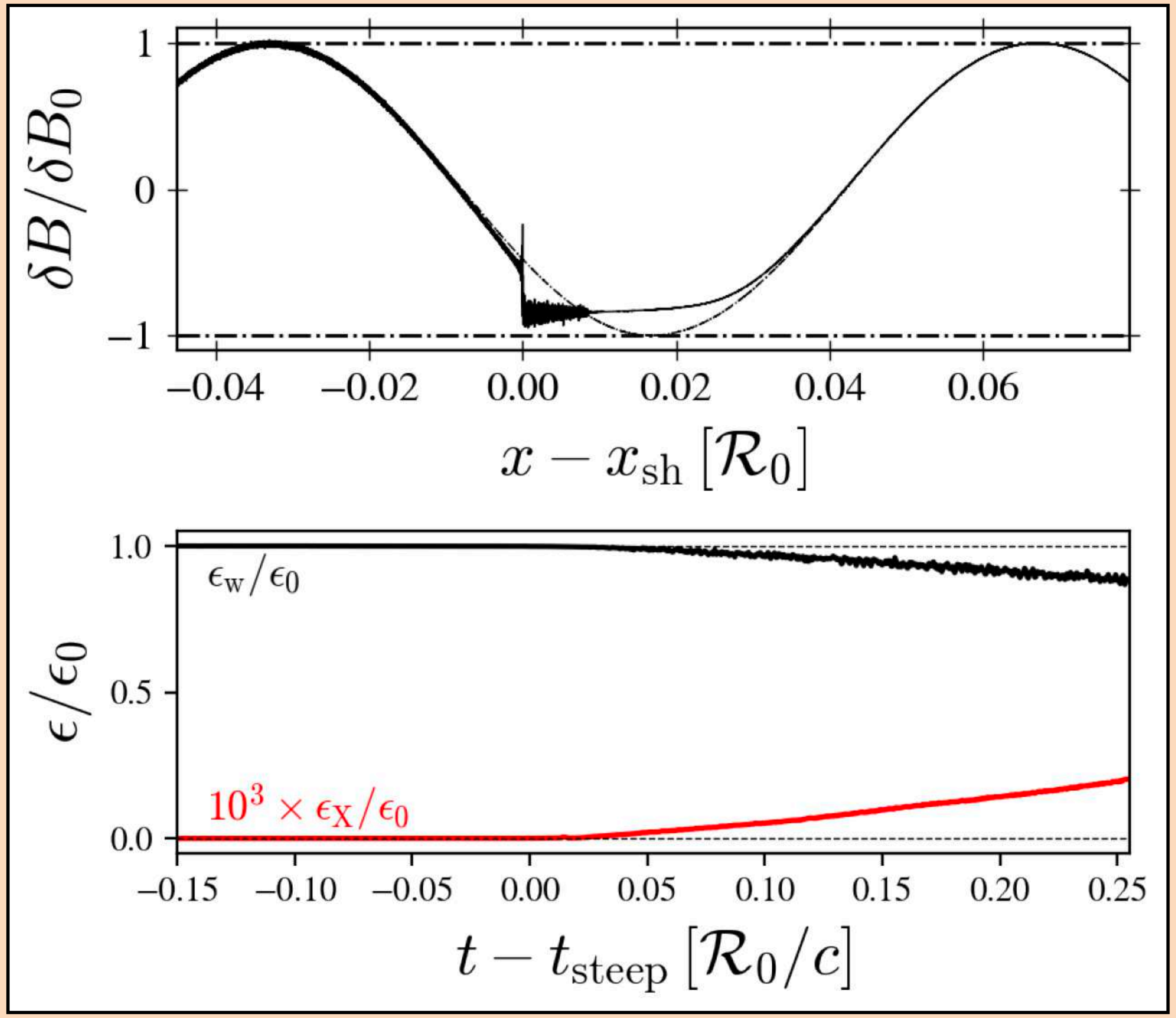

- **Low energy cutoff**: $\partial_k\omega < v_{\rm sh|Lab} \implies \omega_{\rm cut} = \omega_{\rm p}'\gamma_{\rm sh|Lab}$
- **Peak frequency** depends on the size of the resonant cavity

$$\omega_{\rm peak|Lab} \sim \sqrt{\sigma}\,\omega_{\rm p}'$$

- **Fraction of dissipated energy** carried by the X-mode

$$\epsilon_X = 10^{-3}$$

A. Vanthieghem & A. Levinson, PRL, 2025

Application to Fast Radio Bursts

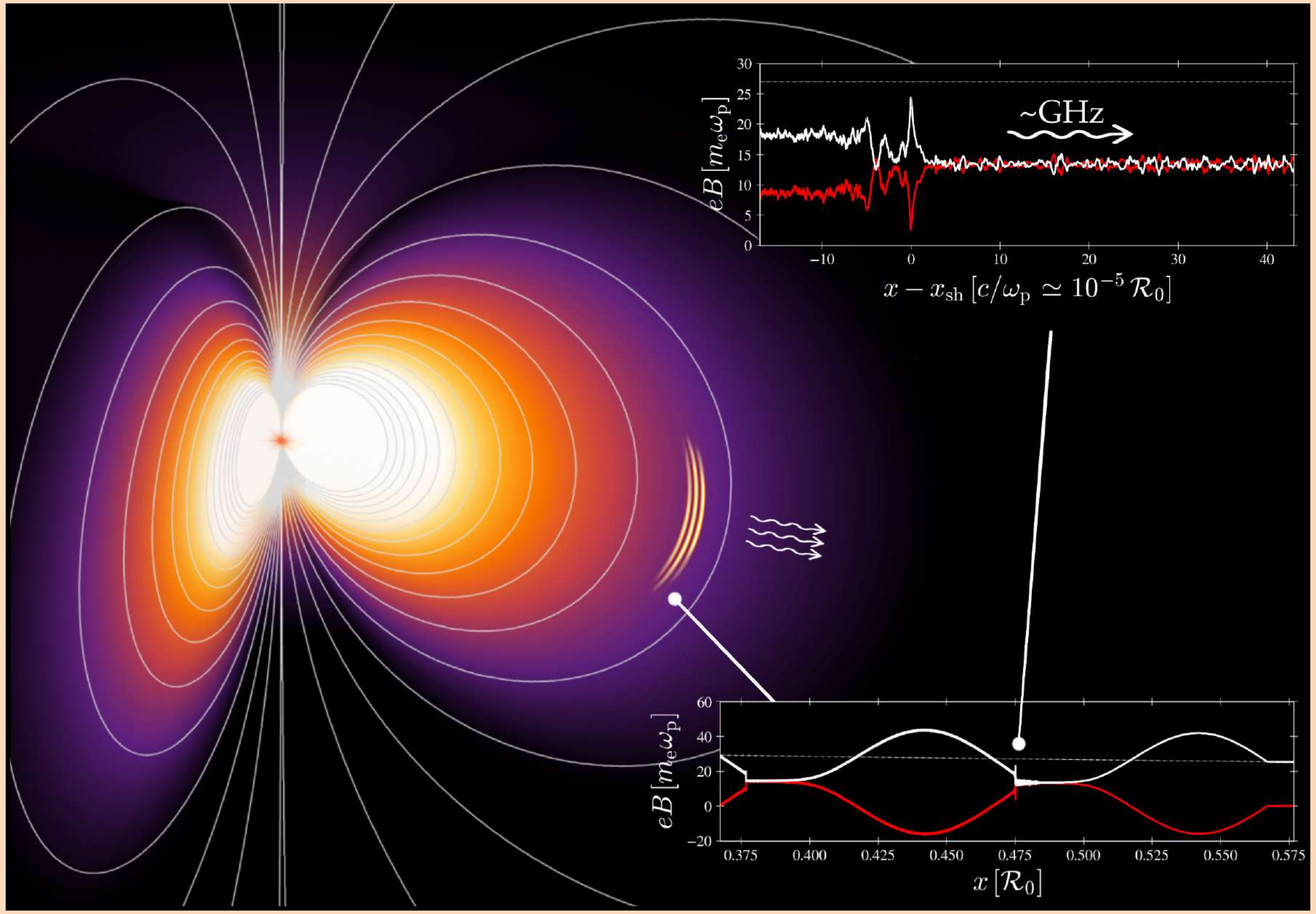

Scalings

- **Shock formation radius**
  $r_s = 2 \times 10^8\, B_{15}^{1/2} L_{43}^{-1/4}$ cm (Beloborodov, 2023)
- **Dissipation zone:** $r_s < r_{diss} < 3r_s$ (Beloborodov, 2023)
- **Upstream magnetization:** $\sigma_u \approx 300\, B_{15}^{1/2} L_{43}^{-1/4}$
- **Plasma frequency:** $\omega_p' = 10^8\,(r/r_s)^{1/2} \mathcal{M}_6 \Omega^{1/2} B_{15}^{1/4} L_{43}^{-1/8}$ Hz
- **Peak emission frequency in the lab frame**
  $\omega_{peak} \simeq \sqrt{\sigma_u}\,\omega_p' \mathcal{M}_6 \sim 2\text{GHz}$
  (scaled from the simulation)

Parameters

- **Dipole**
  $B_{bg} = B_{15}(R/r)^3$
  $R = 10^6\,\text{cm}$
  $\nu = 10^4$ Hz
- **wave power**
  $L_w = 10^{43} L_{43}$ erg/s
- **multiplicity**
  $\mathcal{M} = n_{bg}/n_{GJ} = 10^6 \mathcal{M}_6$
- **FMS wave frequency**
  $\nu = 10^4$ Hz

Open questions:

- Can they escape? Decay into Alfvén waves (Golbraikh & Lyubarsky, 2023), damping (Beloborodov, 2024/2025, Sobacchi et al., 2024)
- Efficiency including radiative cooling? PIC+synchrotron (Zhang et al., 2025)

A. Vanthieghem & A. Levinson, PRL, 2025

A periodic system of solitary structure

Understanding the radiative signature requires a model for the shock structure

- A **quasi-periodic trail** of Fast Magnetosonic Solitons underpins the shock structure

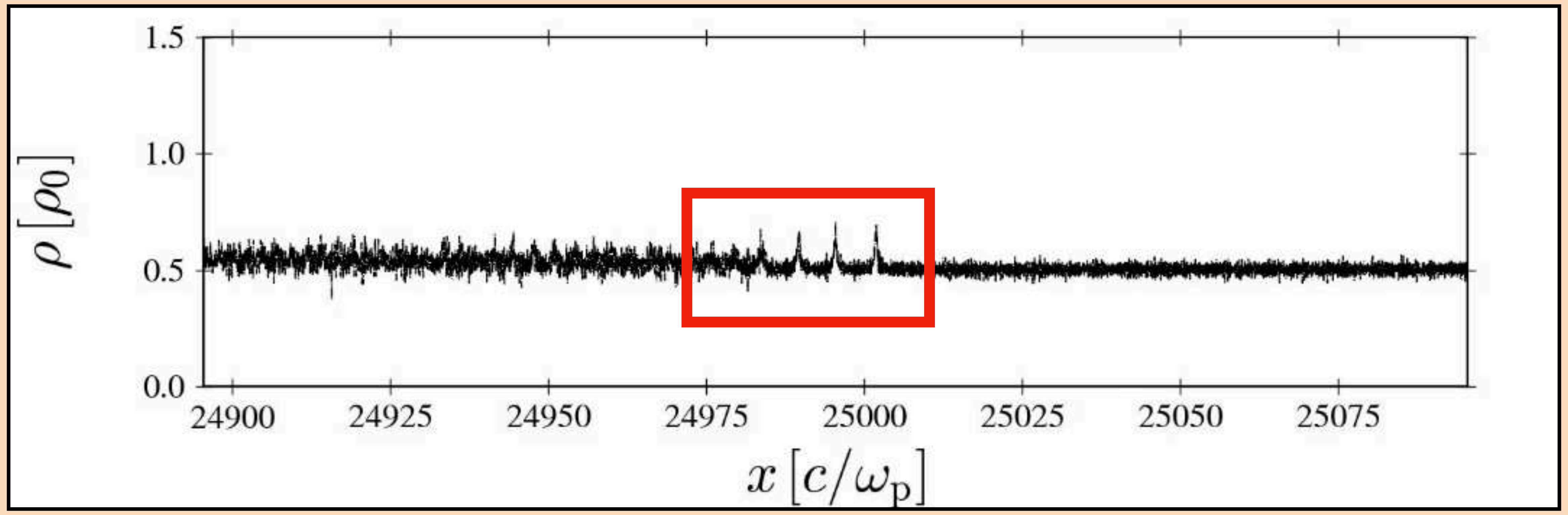

- **A stationary solution from a single fluid + Maxwell's equations**

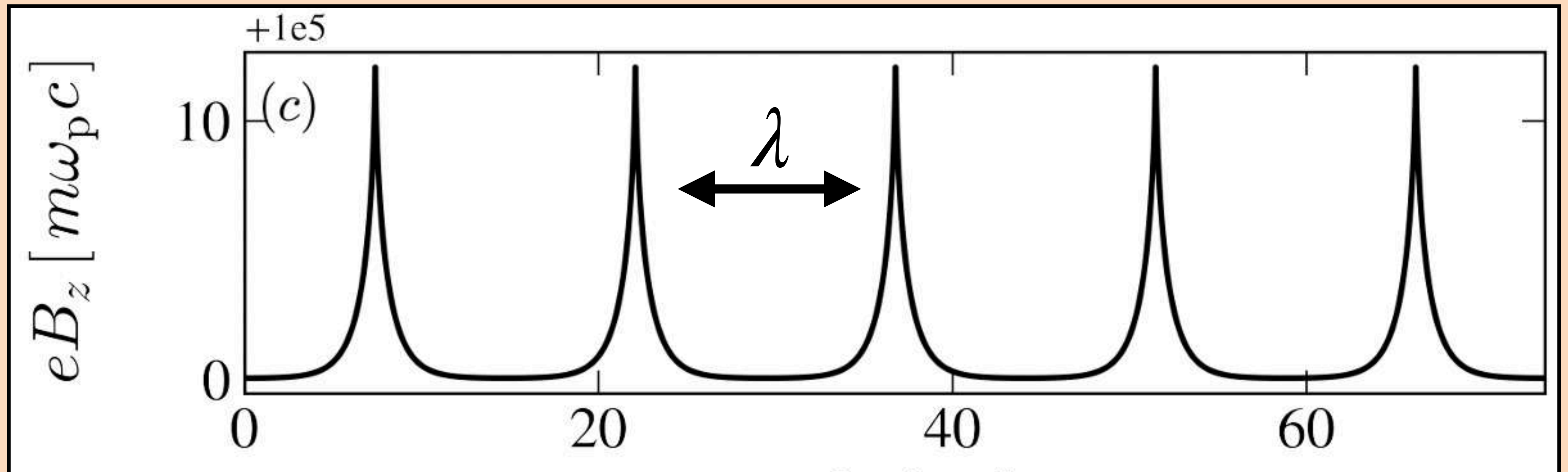

Magnetic field profile

FMS stationary solitons

$$\partial_{\tilde{x}}\tilde{u}_x = \frac{\tilde{B}_z}{M_A}\frac{\tilde{u}_y}{\tilde{u}_x}$$

$$\partial_{\tilde{x}}\tilde{u}_y = -\frac{\tilde{B}_z}{M_A} + \frac{1}{M_A}\frac{\gamma}{\tilde{u}_x}$$

$$\partial_x\tilde{B}_z = -M_A\frac{\tilde{u}_y}{\tilde{u}_x}$$

- Soliton cavity size determines the emission spectral features. The size of the cavity scales weakly with M_A

$$\lambda \sim 2\frac{\ln\left(M_A^2 + \sqrt{M_A^4 - 1}\right)}{\sqrt{1 - M_A^{-2}}}\, c/\omega_p$$

Such that, in the downstream frame, the wavenumber scales as

$$ck_{|d} \sim \gamma_{sh|d}\,\omega_p \sim \sqrt{\sigma}\,\omega_p$$

As observed in PIC simulations (Plotnikov et al., 2018)

A. Vanthieghem & A. Levinson, PRE, 2025

Unstable Test-Particle orbits in a Periodic Trail of solitons

Unstable trajectories in the locally compressed magnetic field

Compressed magnetic field profile

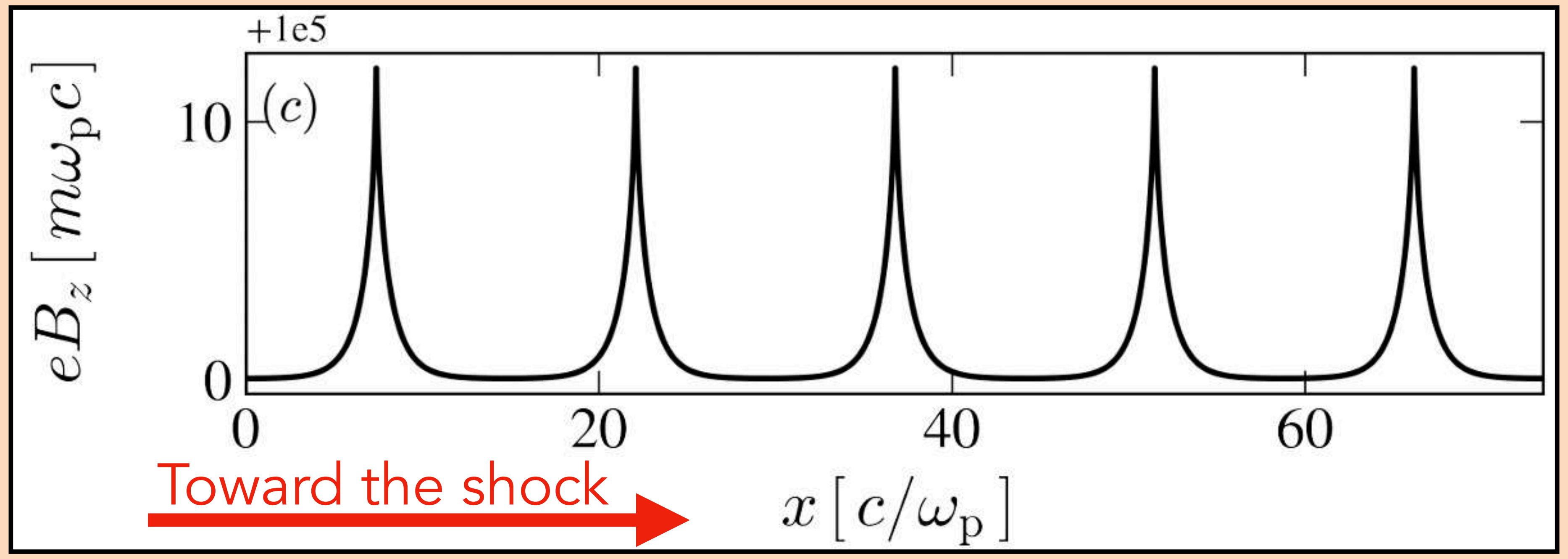

Test-particle phase space trajectories across B_z

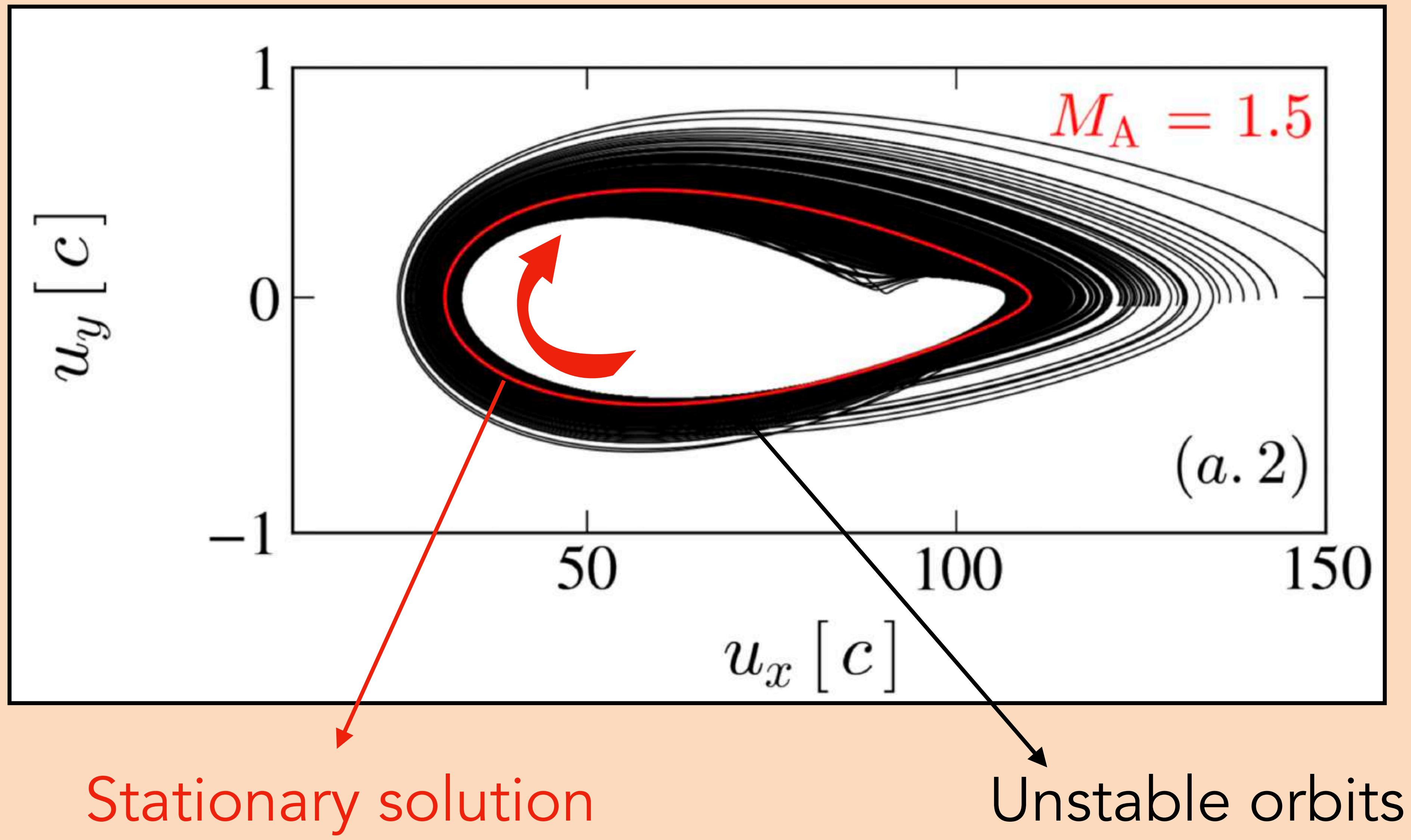

Floquet exponents Γ of the perturbative system with periodic coefficients

$$\begin{cases} \partial_{\tilde{x}}\delta\tilde{u}_x^{(2)} = -\dfrac{\tilde{u}_y}{\tilde{u}_x^2}\dfrac{\tilde{B}_z}{M_A}\delta\tilde{u}_x^{(2)} + \dfrac{\tilde{B}_z}{M_A\tilde{u}_x}\delta\tilde{u}_y^{(2)} \\ \partial_{\tilde{x}}\delta\tilde{u}_y^{(2)} = -\dfrac{1+u_0^2\tilde{u}_y^2}{M_A\tilde{u}_x^2\gamma}\delta\tilde{u}_x^{(2)} + \dfrac{u_0^2}{M_A}\dfrac{\tilde{u}_y}{\tilde{u}_x\gamma}\delta\tilde{u}_y^{(2)} \end{cases}$$

$$\Rightarrow (\delta u_x^{(2)}, \delta u_y^{(2)}) = \sum_{i=1,2}^{2} V_i(x = x+\lambda)\, e^{\Gamma x}$$

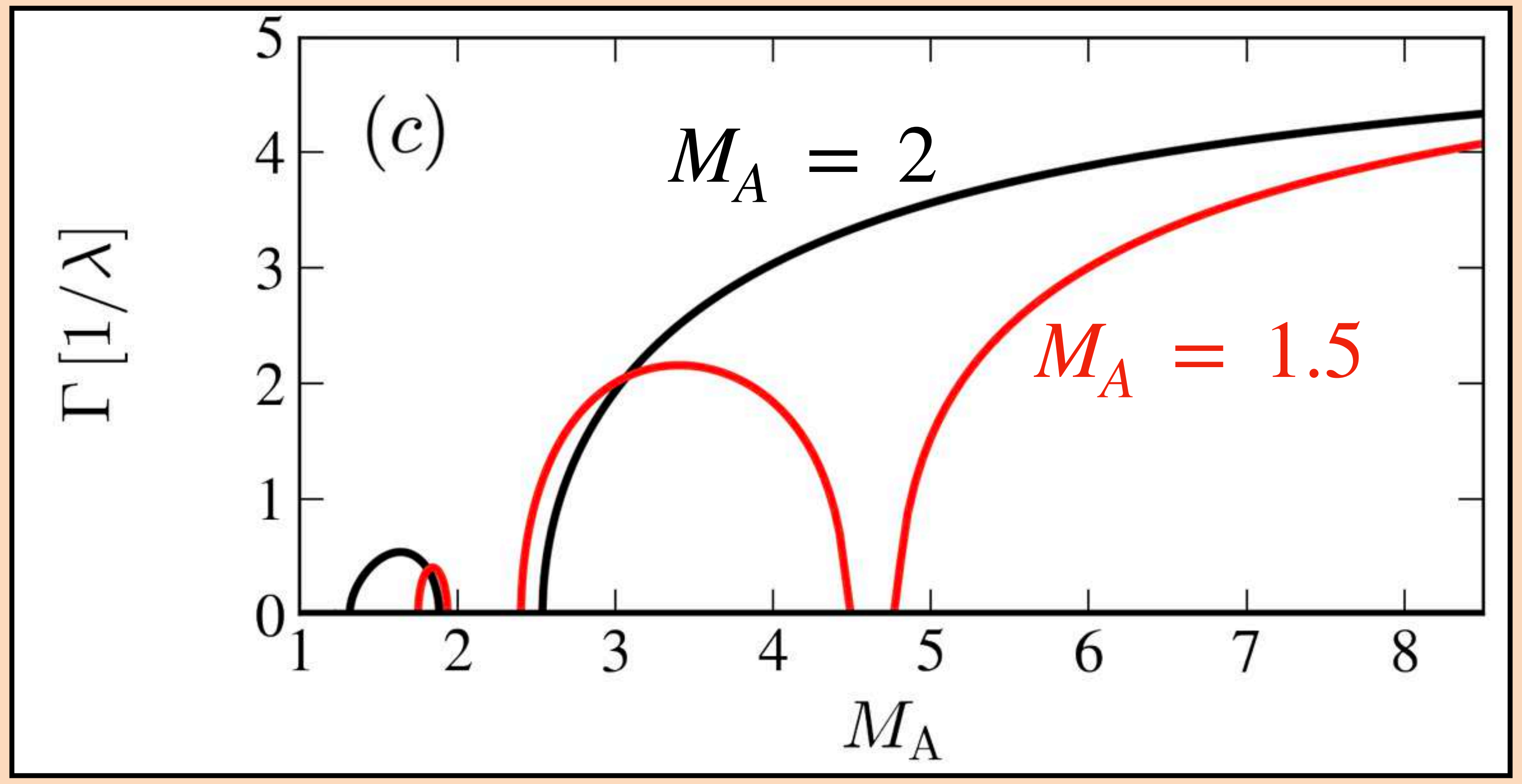

A. Vanthieghem & A. Levinson, PRE, 2025

Self-Consistent coupling with the magnetic field

Observatoire de Paris

$\Longrightarrow$ The **stationary state** is modelled as a **dynamical system of N-fluids** with $N \gg 1$

A reduced model for the steady flow:

- Multi-fluid pair plasma, $i = 1, \ldots, N$
- electron-positron beams as a single fluid (Kennel & Pellat 76, Alsop & Arons 88)
- Initial conditions for the plasma system
    1. Magnetized
    2. Drifting
    3. **Thermal spread**

The multi-fluid (cold) approach captures kinetic effects and convergence with increasing N (Dawson, 1960)

Dynamical system

$$\partial_{\tilde{x}} \tilde{u}_x^i = \frac{\tilde{B}_z}{M_\mathrm{A}} \frac{\tilde{u}_y^i}{\tilde{u}_x^i}$$

$$\partial_{\tilde{x}} \tilde{u}_y^i = -\frac{\tilde{B}_z}{M_\mathrm{A}} + \frac{1}{M_\mathrm{A}} \frac{\gamma^i}{\tilde{u}_x^i}$$

$$\partial_x \tilde{B}_z = -M_\mathrm{A} \frac{1}{N} \sum_i^N \frac{\tilde{u}_y^i}{\tilde{u}_x^i}$$

Longitudinal Velocity **Transverse Velocity** **Magnetic Field**

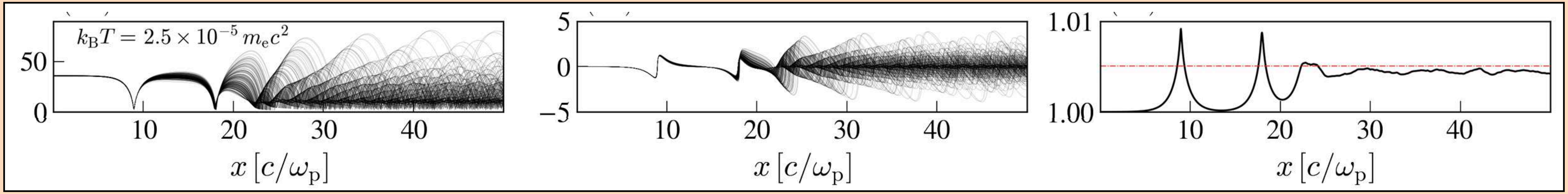

$N = 200$, $\sigma = 100$, $u_0 = 35.8$, and $k_\mathrm{B}T = 2.5 \times 10^{-5}\, m_\mathrm{e}c^2$

A. Vanthieghem & A. Levinson, PRE, 2025

A Model of the Shock Structure

Observatoire de Paris

Kinetic Simulation

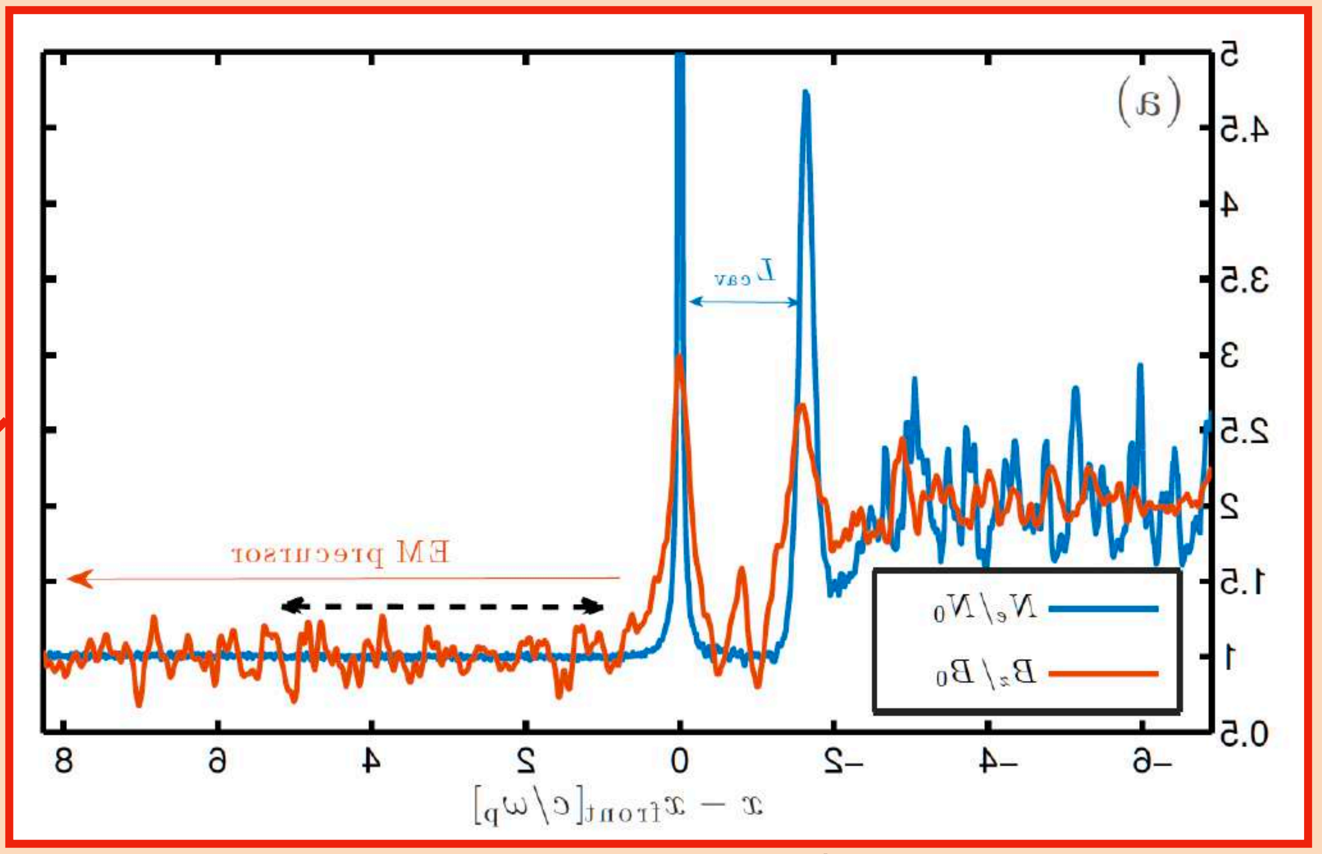

Plotnikov & Sironi, 2019

Theory

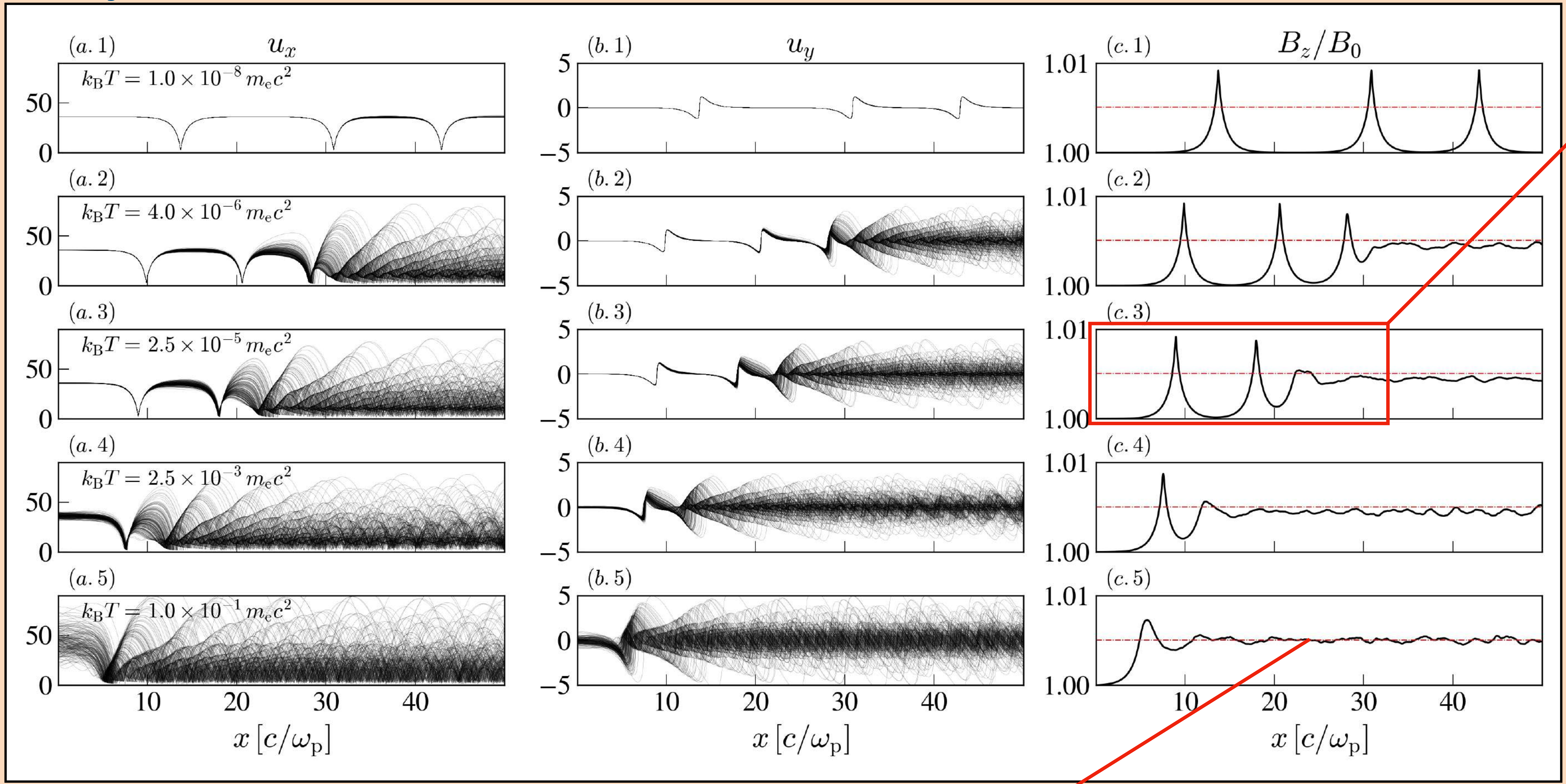

$N = 200$; $\sigma = 100$; $u_0 = 35.8$

Recovered jump conditions

- Increasing temperatures lead reduced number of soliton generations
- At $k_B T = 0.1\, m_e c^2$, the soliton cavity disappears (Babul et al., 20)

A. Vanthieghem & A. Levinson, PRE, 2025

Chaos, Entropie, and Thermalization

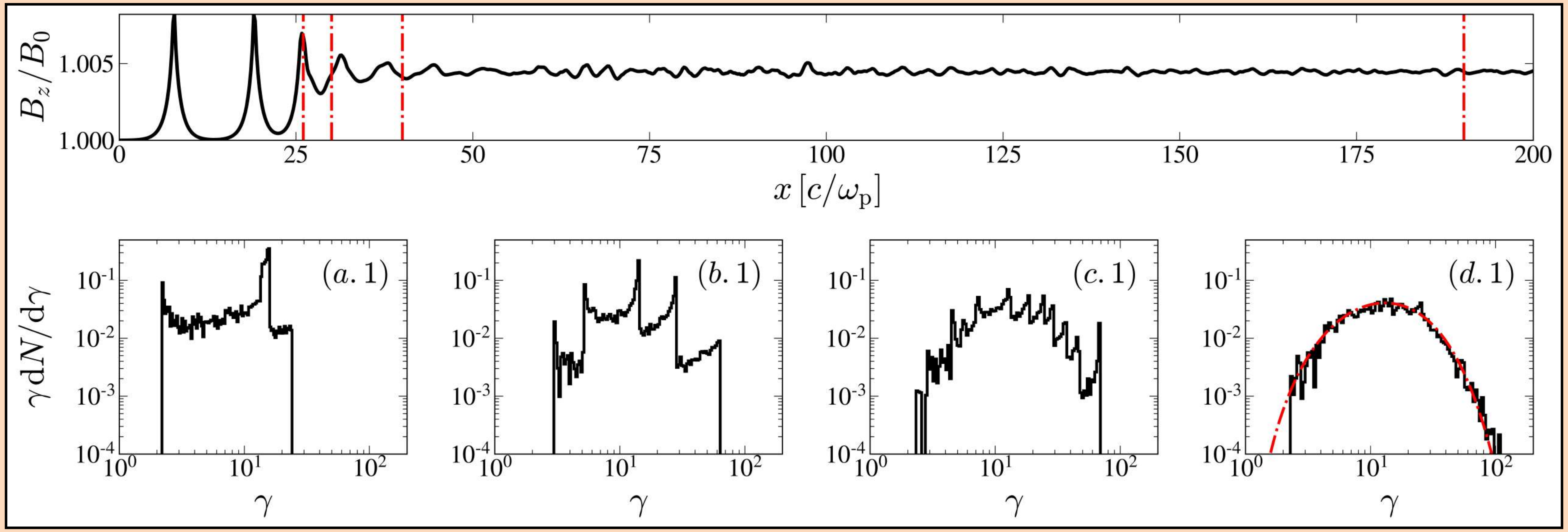

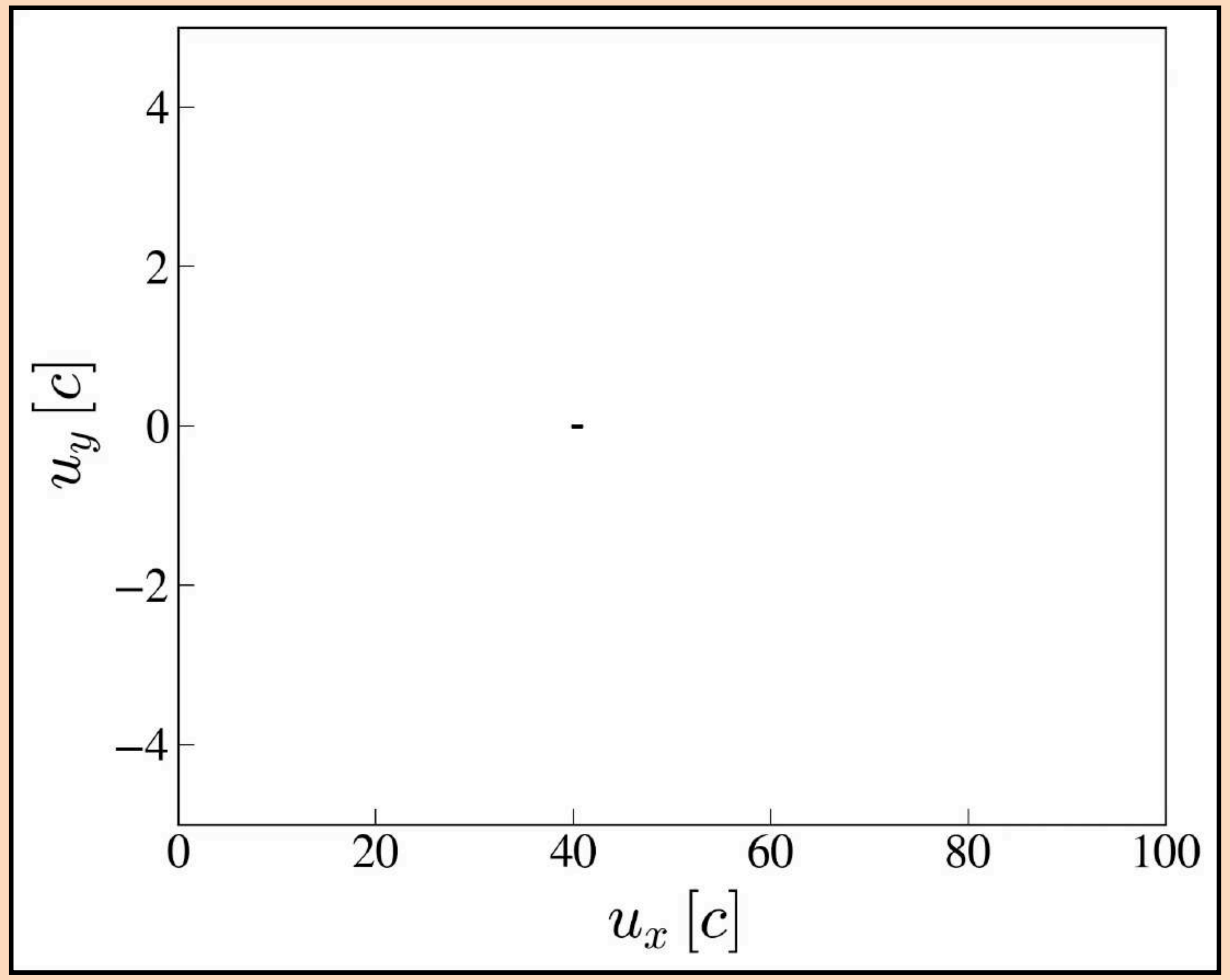

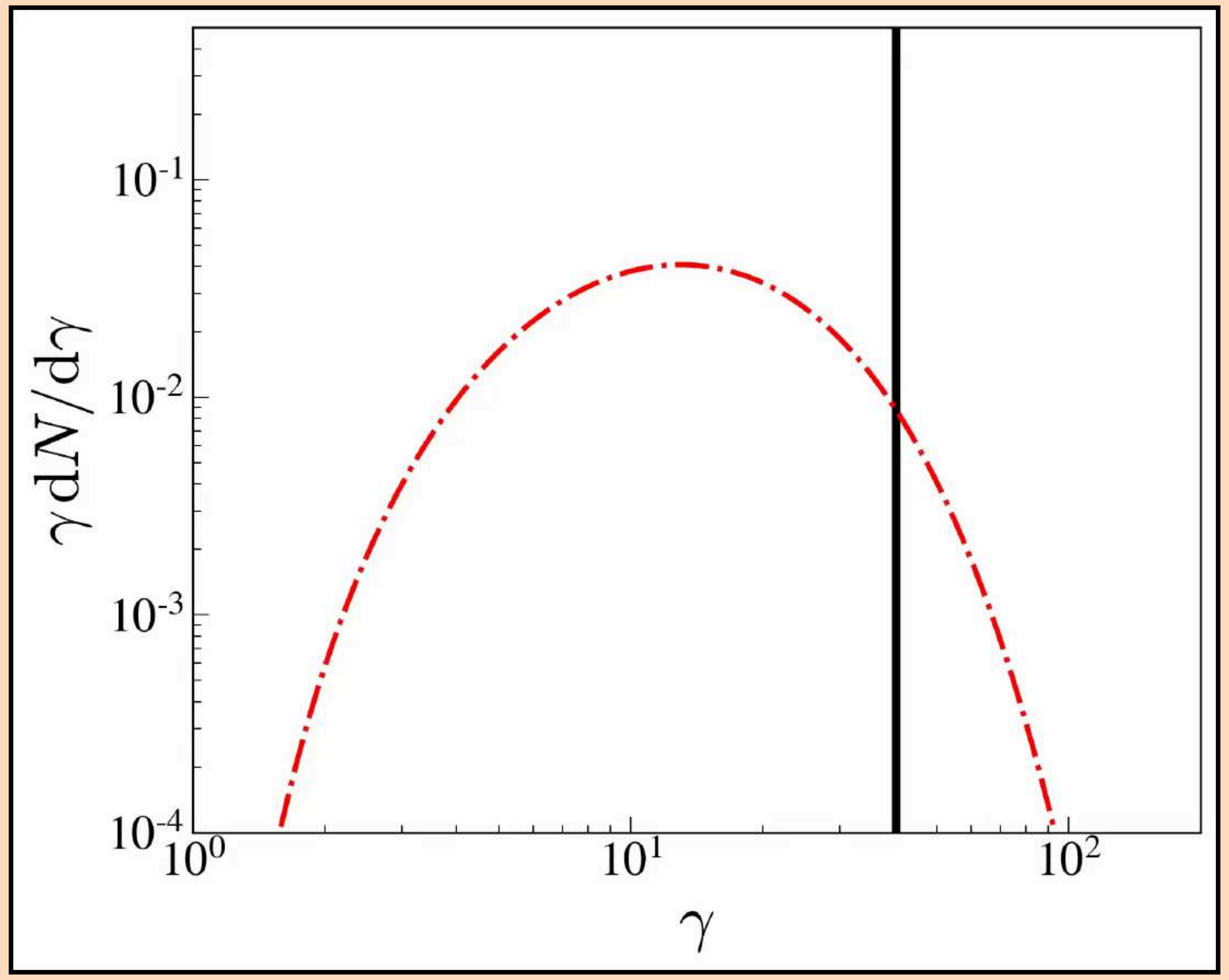

- Phase mixing between fluid trajectories

Full PIC

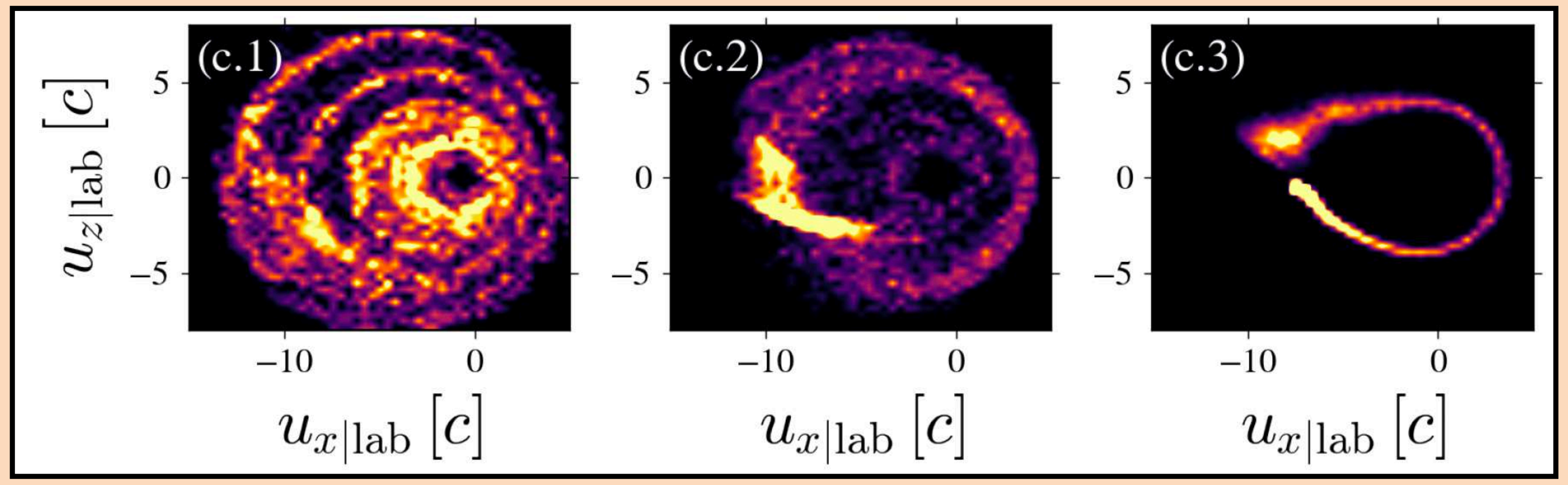

- Downstream thermalization through multiple scattering

A. Vanthieghem & A. Levinson, PRE, 2025

Critical point for soliton stability around $M_A \sim 2$

Observatoire de Paris

The characteristics of the chaotic dynamics are quantified by the set of Lyapunov exponents (divergence rate of trajectories)

$$\mathbf{\Lambda} = \{\Lambda_i \,|\, i = -N, \ldots, 0, \ldots, N\}$$

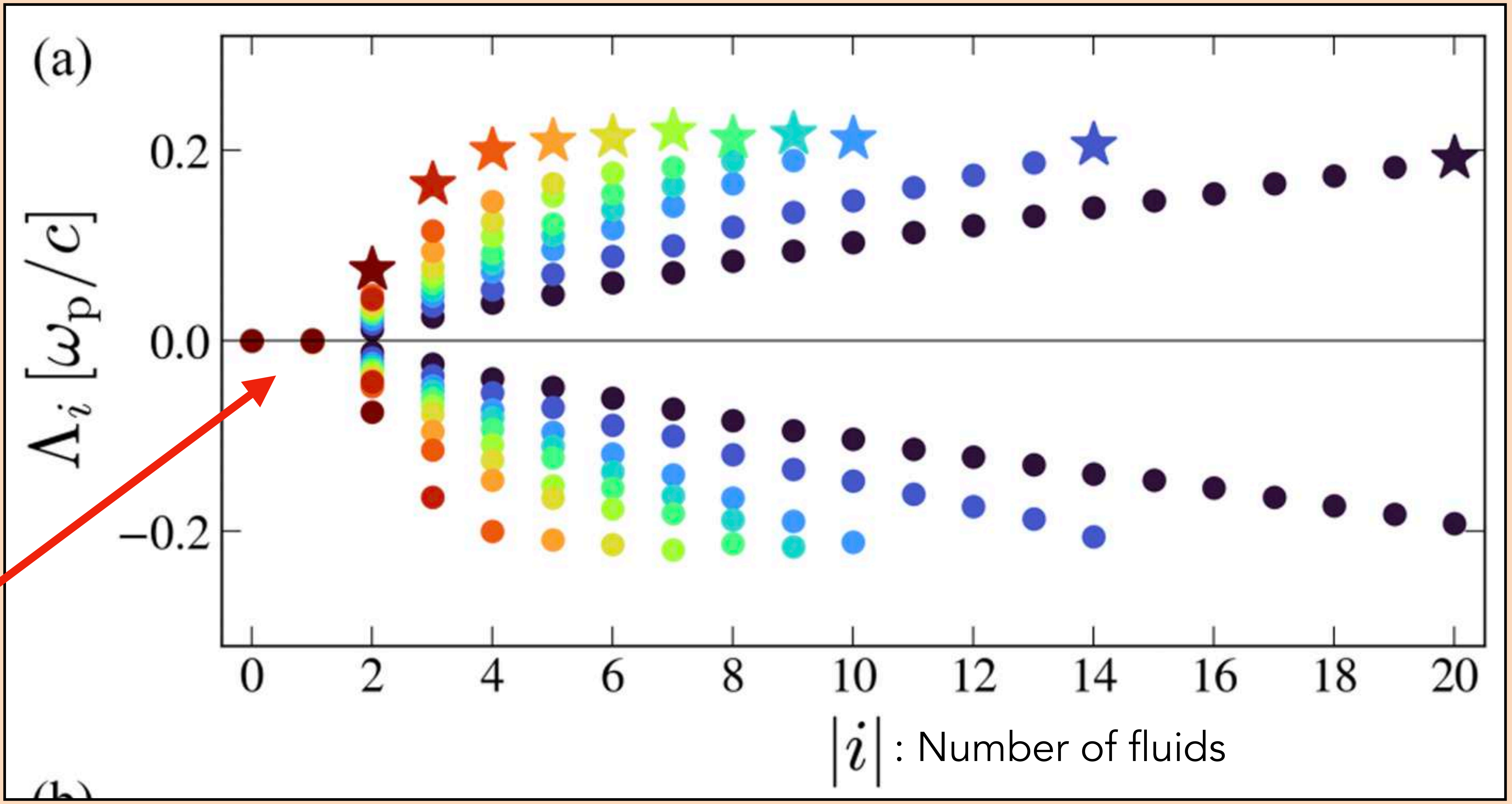

2+1 vanishing Lyapunov exponents:

- 2 integral of motions
- 1 involution: $(u_x, u_y, B_z) \rightarrow (u_x, -u_y, B_z)$

⇒ At least two fluids for the onset of chaos

⇒ Natural interpretation for entropy generation & thermalization scale

A. Vanthieghem & A. Levinson, PRE, 2025

Critical point for soliton stability around $M_A \sim 2$

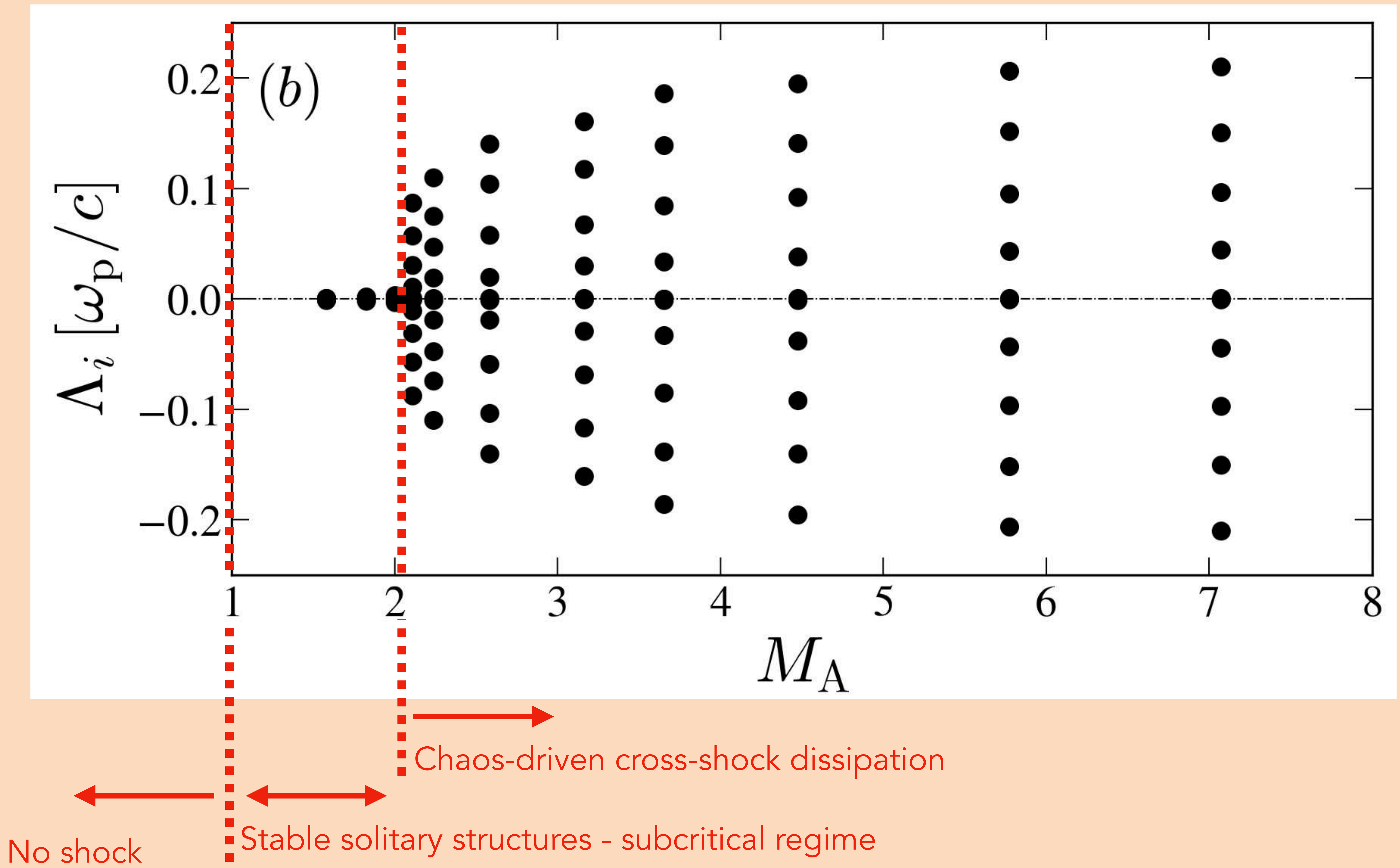

A. Vanthieghem & A. Levinson, PRE, 2025

Subcritical Relativistically Magnetized Shock Waves

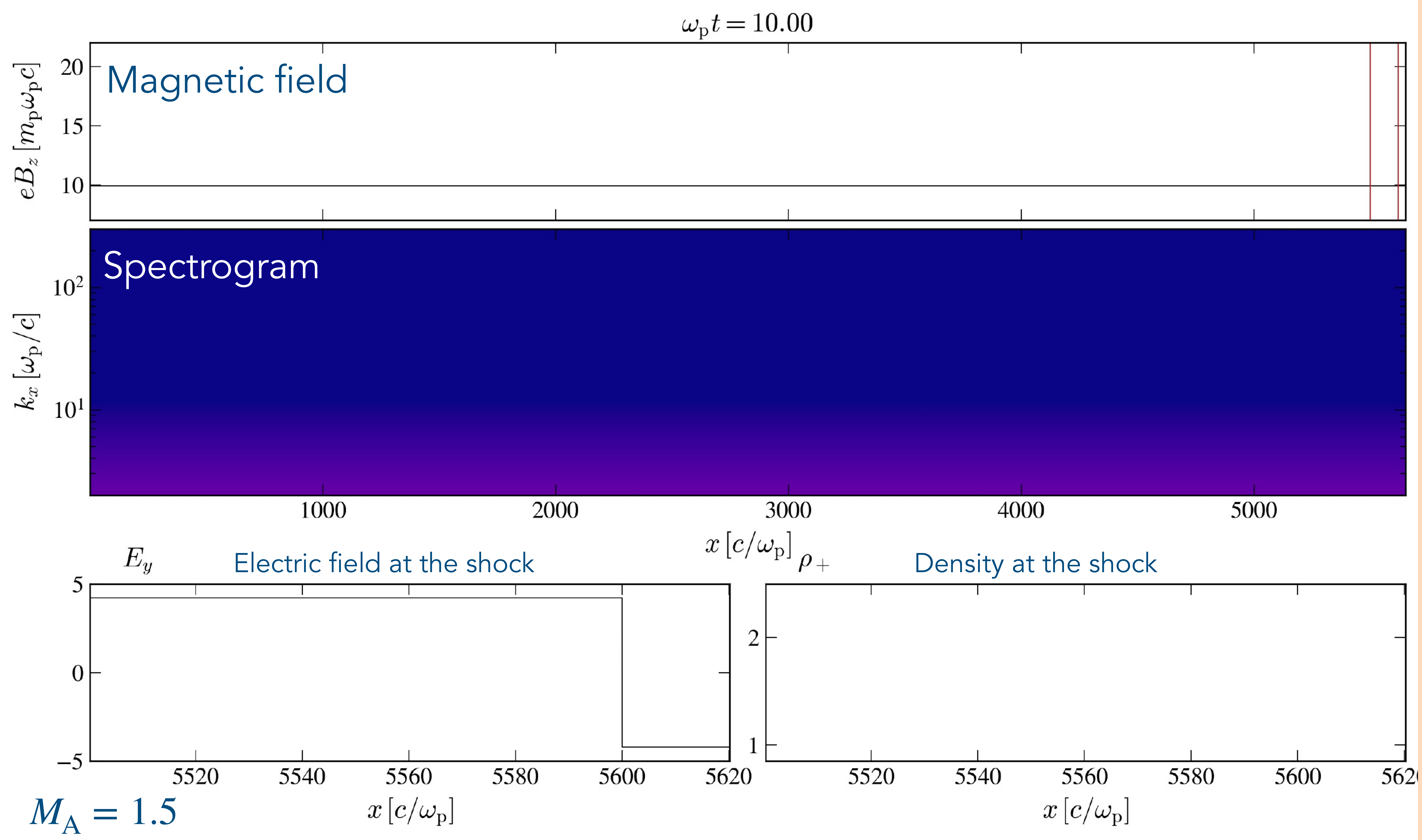

Stable trajectories in solitons lead to inefficient dissipation of the directed kinetic energy across the shock

⇒ **Subcritical shock**

In prep.

Radiation Reaction in Monster Shocks

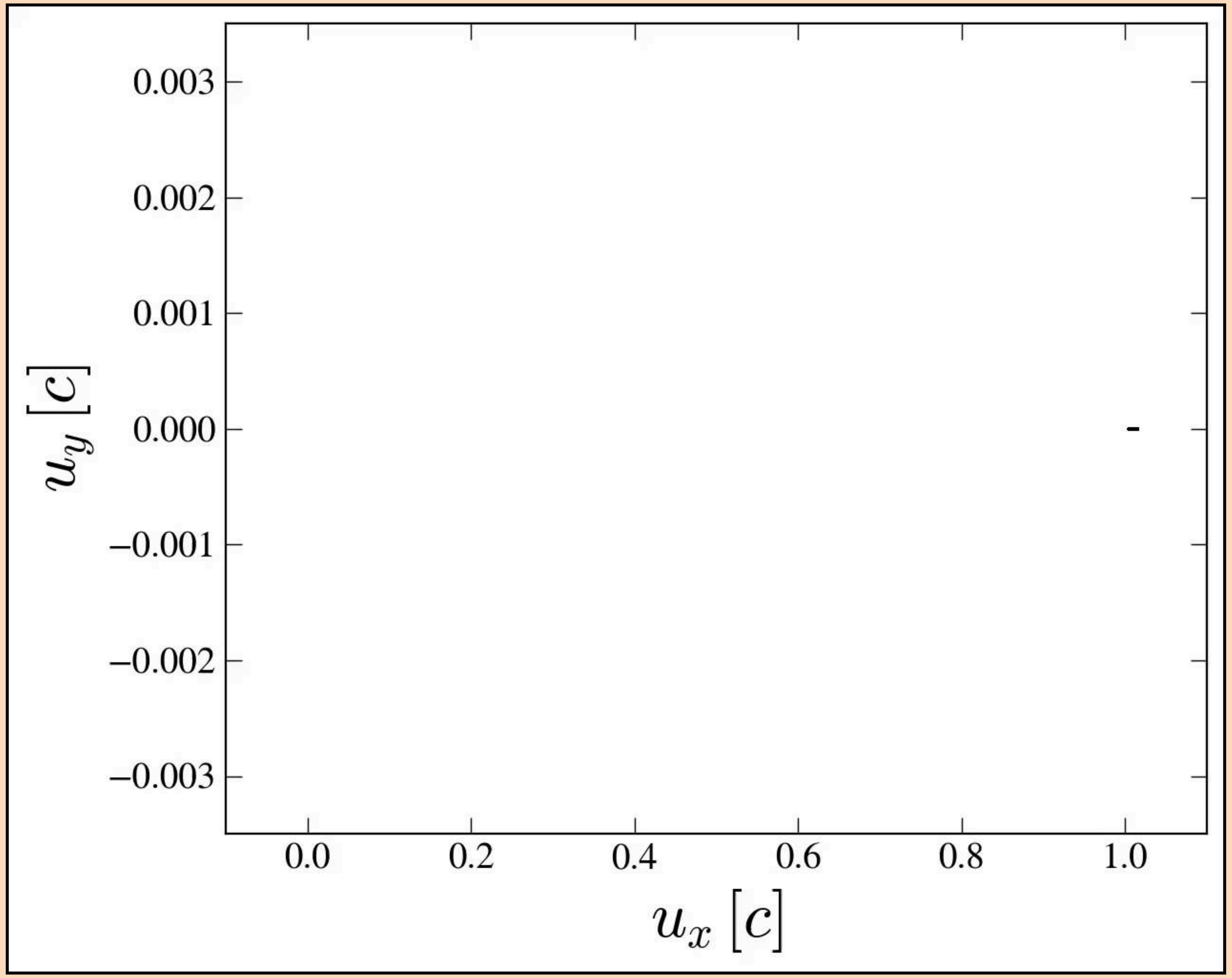

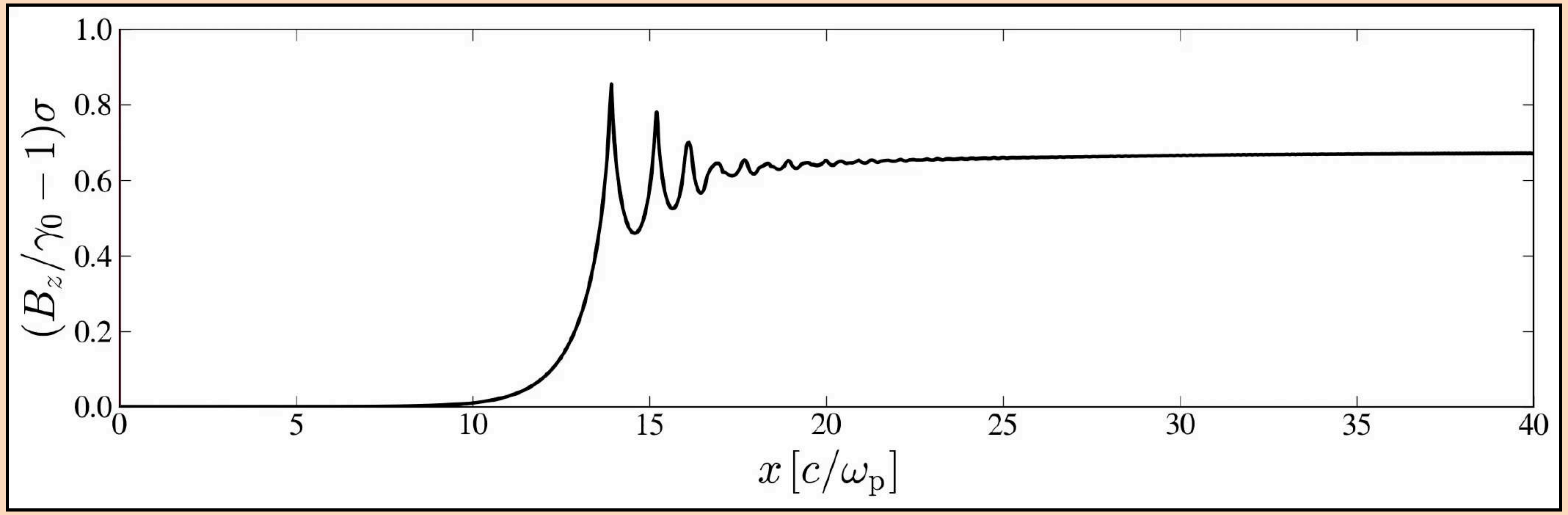

Include radiation reaction

$$\mathscr{F}_\mathrm{rad} = \tau\sigma^2\left(\xi - \frac{\gamma}{u_0}\chi_\mathrm{R}^2\tilde{u}\right)$$

Typical cosmological FRBs are in the strong cooling regime

$$\sigma_T n_p c/\omega_\mathrm{p} \sim 2\times10^{-16}B_{15}^{1/4}L_{43}^{-1/8}\mathscr{M}_6\Omega\nu_4^{1/4}$$

$$u_0 \sim 3\times10^{6}B_{15}^{-1}L_{43}\mathscr{M}_6^{-1}\Omega^{-1}\nu_4^{-1}$$

$$M_\mathrm{A} \sim 2\times10^{5}B_{15}^{-5/4}L_{43}^{9/8}\mathscr{M}_6^{-1}\Omega^{-1}\nu_4^{-1/2}$$

$\Rightarrow \tau \sim 24$

$(L_{43} = 10^{-4} \Rightarrow \tau \sim 10^{-3})$

In prep.

Synchrotron Radiation Reaction in Monster Shocks

Structure of a monster shock with radiation reaction

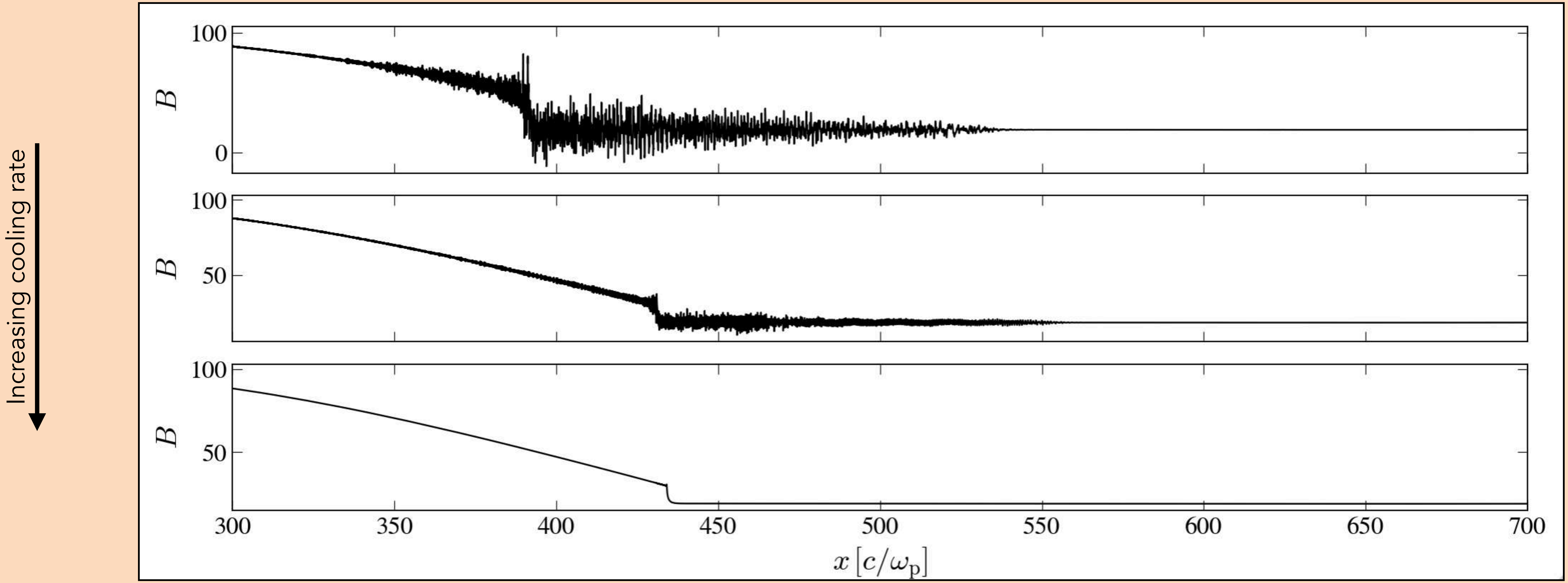

Increasing the cooling rate leads to faster shock, increasing the emission frequency in the FMS wave frame, and may lead to X-mode suppression

In prep.

Conclusion and Perspectives

- Shocks form in a MHD system when $B^2 - E^2 \to 0$
- Shock structure: a quasi-periodic decaying soliton train dictated by $k_B T$ and M_A leading to chaos
- Collective plasma instabilities play a minor role in shock formation
- A general model for the shock structure, including synchrotron cooling

Next

- Obliquity
- Escape